International Journal of Control

ISSN: (Print) (Online) Journal homepage: https://www.tandfonline.com/loi/tcon20

Finite-time stable tracking control for an underactuated system in SE(3) in discrete time

Reza Hamrah & Amit K. Sanyal

To cite this article: Reza Hamrah & Amit K. Sanyal (2020): Finite-time stable tracking control for an underactuated system in SE(3) in discrete time, International Journal of Control, DOI: 10.1080/00207179.2020.1841299

To link to this article: https://doi.org/10.1080/00207179.2020.1841299

Published online: 09 Nov 2020.

INTERNATIONAL JOURNAL OF CONTROL
https://doi.org/10.1080/00207179.2020.1841299

Taylor & Francis
Taylor & Francis Group

Finite-time stable tracking control for an underactuated system in SE(3) in discrete time

Reza Hamrah and Amit K. Sanyal

Department of Mechanical and Aerospace Engineering, Syracuse University, Syracuse, NY, USA

ABSTRACT

We consider tracking control of an underactuated system on the tangent bundle of the six-dimensional Lie group of rigid body motions, SE(3). We formulate a finite-time stable (FTS) tracking control scheme for this underactuated system in discrete time. This scheme is based on our recently developed theory for finite-time stability for discrete-time systems using discrete Lyapunov analysis. The proposed scheme here is developed in discrete time as it is more convenient for onboard computer implementation and ensures stability irrespective of the sampling period. This scheme guarantees a stable convergence of translational and rotational tracking errors to the desired trajectory in finite time. Furthermore, the advantages of finite-time stabilisation in discrete-time over finite-time stabilisation of a sampled continuous-time tracking control system is addressed here through a numerical comparison. This comparison is performed using numerical simulations on continuous and discrete FTS tracking control schemes applied to an unmanned aerial vehicle model.

ARTICLE HISTORY
Received 19 April 2020
Accepted 19 October 2020

KEYWORDS
Geometric control; Lie groups; Lyapunov stability in discrete time; finite-time stability; underactuated system; trajectory tracking

1. Introduction

Unmanned aerial vehicles (UAVs) are finding an increasing set of application such as security, inspection of civilian infrastructure, agriculture and aquaculture, space and underwater exploration, wildlife tracking, package delivery, and remote sensing, all of which can benefit from reliable autonomous operations. Autonomous operations including autonomous trajectory tracking for unmanned vehicles is a challenging problem that has attracted the attention of many researchers, especially in applications where it is difficult or impossible to do remote piloting. The key objective of reliable operations of UAVs is stable and robust guidance and control, particularly for operations that need safety and reliability in the presence of external disturbances.

The literature on tracking control of UAVs includes many linear control methods that fail to work for large manoeuvers due to the nonlinearities in the dynamics. A variety of nonlinear controllers using such methods as sliding-mode, backstepping, dynamic inversion (Wang et al., 2013), and feedback-linearisation (D. Lee et al., 2009), have also been proposed as solutions to this problem. An important issue in control of rigid body systems is the characterisation of the configuration space, and thereby the state space. The configuration space for a rigid body is not a linear (vector) space. Commonly used attitude representations for rigid body rotational dynamics and control are Euler angles on $\mathbb{R}^3$ and unit quaternions on $\mathbb{S}^3$ (the unit hypersphere embedded in $\mathbb{R}^4$). Euler angles are not unique at certain orientations where the angles rates become unbounded, a phenomenon called 'gimbal lock'. Unit quaternions can represent all attitudes, but are ambiguous: an antipodal pair of unit quaternions represent a single attitude. This leads to a type of instability called 'unwinding' in continuous state feedback (Bhat & Bernstein, 2000; Chaturvedi et al., 2011). To avoid the aforementioned drawbacks, geometric control methods have been used for control of UAVs. An early work using geometric control on Lie groups to treat the trajectory tracking problem for a fully-actuated system on SE(3) was presented in Bullo and Murray (1999), which generalised the classical proportional derivative (PD) control in a coordinate-free way. Geometric tracking controllers based on the special Euclidean group SE(3) that avoid singularities and instabilities of other control laws, were reported in Shi et al. (2015), T. Lee et al. (2010, 2012), Mellinger and Kumar (2011), Kushleyev et al. (2013), Rudin et al. (2011), Fernando et al. (2011), H. Lee et al. (2013), Goodarzi et al. (2015), and Invernizzi and Lovera (2017). It is worth mentioning that all these controllers are obtained in continuous time.

This work presents a systematic treatment of *discrete-time* stable geometric control for tracking position and attitude trajectories of unmanned vehicles that have four independent control inputs for the six degrees of freedom of translational and rotational motion in three dimensional Euclidean space. The control inputs actuate the three degrees of rotational motion and one degree of translational motion in a vehicle body-fixed coordinate frame. This actuation model covers a wide range of unmanned vehicles like fixed-wing and rotorcraft

CONTACT Reza Hamrah rhamrah@syr.edu; Amit K. Sanyal aksanyal@syr.edu Department of Mechanical and Aerospace Engineering, Syracuse University, Syracuse, NY 13244, USA
This article has been republished with minor changes. These changes do not impact the academic content of the article.

unmanned aerial vehicles, underwater vehicles, and spacecraft. The advantages of the tracking control laws proposed here are two-fold: they are finite-time stable, and they are obtained in discrete-time, which makes it easy for onboard computation implementation.

Finite-time stability: Finite-time stable control has the advantage of providing guaranteed convergence to a desired state (or trajectory) in finite time, as well as being more robust to bounded temporary and persistent disturbances than asymptotic stability. Furthermore, low-level persistent disturbances are better rejected by a finite-time stable system in comparison to an asymptotically stable system, because the ultimate bound on the state is of higher order than the bound on the disturbance (Sanyal & Bohn, 2015). A finite-time stable control scheme for simple mechanical systems in generalised coordinates is designed and presented in Sanyal and Bohn (2015). In Sanyal et al. (2013), continuous finite-time stable control (FTS) schemes are shown to be effective, especially when there are bounded disturbance inputs. Continuous FTS control systems have been analysed in Shi et al. (2015), Bhat and Bernstein (1998, 2000), Dorato (2006), Haddad et al. (2008), Yan et al. (2015), and Harshavarthini et al. (2019). An almost global finite-time stabilisation of rigid body attitude motion to the desired attitude is studied in Sanyal et al. (2013) and Bohn and Sanyal (2015). Continuous-time FTS integrated guidance and feedback tracking control schemes for pose tracking of rigid bodies were reported in Prabhakaran et al. (2018), Prabhakaran, Sanyal, and Izadi (2017), and Prabhakaran, Sanyal, and Warier (2017), which ensure finite-time stability of the overall feedback system. In these papers, the continuous equations of motion were discretised in the form of a Lie Group Variational Integrator (LGVI) by applying the discrete Lagrange–d'Alembert principle, and the continuous-time control scheme was sampled at a constant trajectory for computer implementation. Prior related research on LGVI discretisation of rigid body dynamics includes (Hussein et al., 2006; Izadi & Sanyal, 2014, 2016; T. Lee et al., 2005; Marsden & West, 2001; Nordkvist & Sanyal, 2010; Sanyal et al., 2011).

Discrete-time stability: Implementing a sampled continuous-time stable tracking control scheme does not ensure discrete-time stability of the resulting feedback system. This was indicated for the case of nonlinear observer design for attitude dynamics, in Izadi and Sanyal (2014, 2016), and Izadi et al. (2015). A discrete-time stable feedback tracking control scheme was developed in Hamrah et al. (2018), in which discrete-time control laws obtained guaranteed asymptotic discrete-time stability of pose tracking control of underactuated vehicles on SE(3). Note that, like the continuous-time FTS control schemes in above-cited work, the discrete-time FTS control scheme proposed here guarantees finite-time stable convergence to the desired equilibrium or trajectory, but it does so in discrete time. In addition, discrete-time FTS control scheme enables onboard computer implementation with a variety of discrete-time input data frequencies. A finite-time stable position tracking controller and an attitude tracking control scheme are presented in Hamrah et al. (2019, 2020), respectively. This paper integrates these two FTS tracking controllers to form a finite-time stable pose tracking control scheme in SE(3) in discrete-time, which is the first of its kind. A finite-time stabilisation scheme in discrete-time is formulated here for pose tracking in SE(3), using discrete-time Lyapunov analysis which leads to the discrete-time control law. This discrete-time control law ensures position and attitude trajectory tracking errors converge to zero in a finite-time interval. The stability and performance of the proposed discrete FTS scheme control are numerically compared with those of a continuous FTS scheme, and the results are discussed.

The remainder of this paper is organised as follows. Section 2 outlines the general formulation of the problem for a rigid body on SE(3), as well as providing the tracking error kinematics and dynamics of the vehicle and their discretisations. Section 3 presents a basic result on finite-time stability and convergence for discrete-time systems. Sections 4 and 5 deals with the discrete-time Lyapunov framework and a two-step systematic method to obtain discrete-time position and attitude tracking control laws for FTS pose tracking control in SE(3), respectively. A continuous FTS tracking scheme is provided in Section 7, which is the scheme first proposed in Prabhakaran et al. (2018). Numerical simulation results based on a Lie group variational integration scheme and the finite-time control laws obtained in discrete time are presented in Section 8. This section also presents a comparison of the stability properties of the discrete-time and continuous-time FTS schemes. The concluding Section 9 gives a summary of the presented results and mentions related research directions to be pursued in the near future.

2. Problem formulation

2.1 Coordinate frame definition

The configuration of an unmanned vehicle modelled as a rigid body is given by its position and orientation, which are together referred to as its pose. To define the pose of the vehicle, we fix a coordinate frame $\mathcal{B}$ to its body and another coordinate frame $\mathcal{I}$ that is fixed in space and takes the role of an inertial coordinate frame. Let $b \in \mathbb{R}^3$ denote the position vector of the origin of frame $\mathcal{B}$ with respect to frame $\mathcal{I}$ represented in frame $\mathcal{I}$. Let $R \in$ SO(3) denote the orientation (attitude), defined as the rotation matrix from frame $\mathcal{B}$ to frame $\mathcal{I}$. The pose of the vehicle can be represented in matrix form as follows:

$$g = \begin{bmatrix} R & b \\ 0 & 1 \end{bmatrix} \in \mathrm{SE}(3), \tag{1}$$

where SE(3) is the six-dimensional Lie group of rigid body motions (translational and rotational) that is obtained as the semi-direct product of $\mathbb{R}^3$ with SO(3) (Varadarajan, 1984). A conceptual diagram of guidance on SE(3) through a set of waypoints is given in Figure 1.

2.2 Trajectory generation for underactuated vehicle

The trajectory generation problem consists of creating an appropriately smooth position trajectory that is continuous and twice differentiable. Such a time trajectory for the position through given waypoints could be generated using one of several techniques (T. Lee et al., 2010; Mellinger et al., 2012). Once the desired position trajectory over time has been generated for

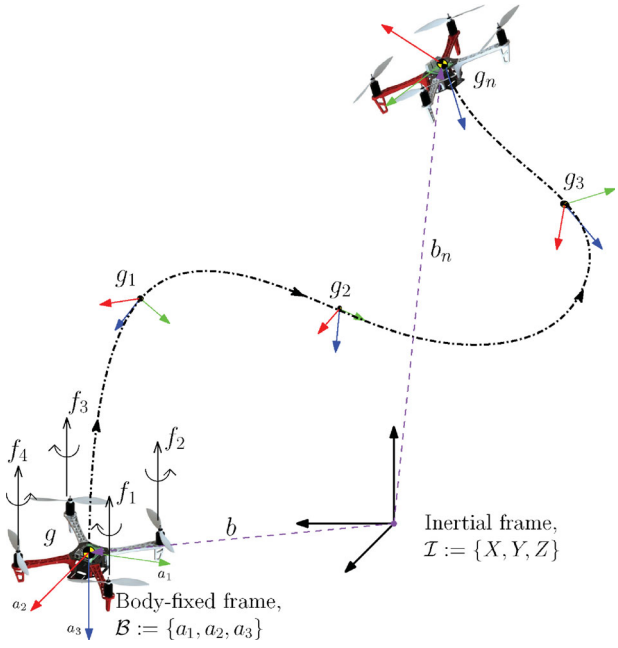

Figure 1. Guidance through a set of finite waypoints between initial and final configurations on SE(3).

the underactuated vehicle with body-fixed thrust direction, a desired attitude trajectory $R^d(t)$ is generated such that the position trajectory is tracked.

Let $g^d(t) \in \mathrm{SE}(3)$ be the desired pose (position and attitude) generated by the guidance scheme (Prabhakaran, Sanyal, & Izadi, 2017; Prabhakaran et al., 2018). Then the desired velocities (translational and rotational) are given by $\xi^d(t)$ that satisfies the kinematics

$$\begin{aligned} \dot{g}^d(t) &= g^d(t)\xi^d(t)^\vee, \quad \text{with} \\ (\xi^d)^\vee &= \begin{bmatrix} (\Omega^d)^\times & \nu^d \\ 0 & 0 \end{bmatrix} \in \mathfrak{se}(3) \subset \mathbb{R}^{4\times 4} \quad \text{for} \\ \xi^d &= \begin{bmatrix} \Omega^d \\ \nu^d \end{bmatrix} \in \mathbb{R}^6. \end{aligned} \tag{2}$$

Here, ν^d, Ω^d are the body's desired translational and angular velocities, respectively, and $(\cdot)^\times : \mathbb{R}^3 \to \mathfrak{so}(3) \subset \mathbb{R}^{3\times 3}$ is the skew-symmetric cross-product operator giving the vector space isomorphism between $\mathbb{R}^3$ and $\mathfrak{so}(3)$:

$$x^\times = \begin{bmatrix} x_1 \\ x_2 \\ x_3 \end{bmatrix}^\times = \begin{bmatrix} 0 & -x_3 & x_2 \\ x_3 & 0 & -x_1 \\ -x_2 & x_1 & 0 \end{bmatrix}. \tag{3}$$

2.3 Tracking error kinematics and dynamics in continuous time

Define pose and desired pose of the vehicle on SE(3) as follows:

$$g = \begin{bmatrix} R & b \\ 0 & 1 \end{bmatrix}, \quad g^d = \begin{bmatrix} R^d & b^d \\ 0 & 1 \end{bmatrix}. \tag{4}$$

Tracking error on SE(3) is given by

$$h = (g^d)^{-1} g = \begin{bmatrix} Q & x \\ 0 & 1 \end{bmatrix}, \tag{5}$$

where

$$Q = (R^d)^{\mathrm{T}} R \tag{6}$$

is the attitude tracking error, and $x = (R^d)^{\mathrm{T}}(b - b^d) = (R^d)^{\mathrm{T}}\tilde{b}$ is the position tracking error, both in the desired body fixed frame. Therefore, the kinematics for the pose tracking error is

$$\dot{h} = h\bar{\xi}^\vee, \tag{7}$$

where

$$\bar{\xi}^\vee = \begin{bmatrix} \omega^\times & \upsilon \\ 0 & 0 \end{bmatrix} \tag{8}$$

and

$$\omega = \Omega - Q^{\mathrm{T}}\Omega^d \tag{9}$$

is the angular velocity tracking error, and $\upsilon = \nu - Q^{\mathrm{T}}(\nu^d + (\Omega^d)^\times x)$ is the translational velocity tracking error expressed in the body frame. The tracking errors for translational motion are expressed with respect to inertial frame as $\tilde{b} := b - b^d$ and $\tilde{\nu} := \nu - \nu^d$, which are position and velocity tracking errors, respectively.

Therefore, in inertial frame $\mathcal{I}$, the translational error dynamics are expressed as

$$\dot{\tilde{b}} = \tilde{\nu} = \nu - \nu^d, \tag{10}$$

$$m\dot{\tilde{\nu}} = mg\,e_3 - (\varphi + \varphi_D) - \nu^d, \tag{11}$$

where m is the mass of rigid body, g is the gravity, φ is the control force vector, and φ_D is the disturbance force vector acting on the body, expressed in inertial frame. The magnitude of this vector is the control input f, which is designed as a feedback control law, and $e_3 = [0\ \ 0\ \ 1]^{\mathrm{T}}$ is the third standard basis of $\mathbb{R}^3$. The position trajectory control law gives a desired thrust direction, which is then used to generate a desired attitude trajectory, as described in Prabhakaran et al. (2018). Let J denote inertia of a rigid body. The rotational dynamics of the rigid body is given by

$$\dot{R} = R\,\Omega^\times, \tag{12}$$

$$J\dot{\Omega} = J\Omega \times \Omega + \tau + \tau_D. \tag{13}$$

where τ is the input torque, and τ_D is an unknown bounded disturbance torque. Therefore, the dynamics for the attitude tracking error is

$$J\dot{\omega} = \tau + J(\omega^\times Q^{\mathrm{T}}\Omega^d - Q^{\mathrm{T}}\dot{\Omega}^d) - (\omega + Q^{\mathrm{T}}\Omega^d)^\times J(\omega + Q^{\mathrm{T}}\Omega^d). \tag{14}$$

Since the translational error dynamics is expressed in the inertial frame, the rotational error dynamics is decoupled from the translational error dynamics such that the translation control force, f, is obtained in the inertial frame followed by the appropriate attitude control, τ, in body frame to track the desired trajectory, b^d.

2.4 Tracking error kinematics and dynamics in discrete time

Consider tracking a desired pose $g^d(t)$ in a time interval $[t_0, t_f] \in \mathbb{R}^+$ separated into N equal-length sub-intervals $[t_k, t_{k+1}]$ for $k = 0, 1, \ldots, N$, with $t_N = t_f$ and $t_{k+1} - t_k = \Delta t$ where Δt is the time step size. Therefore, one can express the discrete-time pose error kinematics and dynamics of an underactuated vehicle in the form of LGVI presented in Nordkvist and Sanyal (2010) and Hamrah et al. (2018) as

$$\begin{cases} \tilde{b}_{k+1} - \tilde{b}_k = \tilde{v}_k \Delta t, \\ m\tilde{v}_{k+1} = m\, v_k + \Delta t\, m\, g\, e_3 - (\bar{\varphi}_k + \bar{\varphi}_k^D) - m v_{k+1}^d, \\ R_{k+1} = R_k\, F_k, \\ J\,\Omega_{k+1} = F_k^{\mathrm{T}} J \Omega_k + u_k + u_k^D, \end{cases} \tag{15}$$

where $v_{k+1} = \tilde{v}_{k+1} + v_{k+1}^d$, $\bar{\varphi}_k = \Delta t \varphi_k$ is the force control input, $\bar{\varphi}_k^D$ is the disturbance force, $u_k = \Delta t \tau_k$ is the torque control input, u_k^D is the disturbance moment in addition to the control torque u_k, and $F_k \approx \exp(\Delta t\, \Omega_k^{\times}) \in \mathrm{SO}(3)$ guarantees that R_k evolves on SO(3). Using the discretised rotational kinematics equation given in (15) and attitude racking error of (6) in discrete form, one can write

$$Q_{k+1} = (R_{k+1}^d)^{\mathrm{T}} R_{k+1} = (R_{k+1}^d)^{\mathrm{T}} R_k\, F_k, \tag{16}$$

where $R_{k+1}^d = R_k^d\, F_k^d$. Then,

$$\begin{aligned} Q_{k+1} &= (F_k^d)^{\mathrm{T}} (R_k^d)^{\mathrm{T}} R_k\, F_k \\ &= (F_k^d)^{\mathrm{T}} Q_k\, F_k. \end{aligned} \tag{17}$$

Using the definitions for F_k and F_k^d given earlier into the above expression and carrying out some algebraic simplifications, one obtains

$$\begin{aligned} Q_{k+1} &\approx Q_k \big[I + \Delta t (\Omega_k - Q_k^{\mathrm{T}} \Omega_k^d)^{\times} \big] \\ &= Q_k (I + \varpi_k{}^{\times}), \end{aligned} \tag{18}$$

where $\varpi_k = \Delta t\, \omega_k$, and ω_k is the angular velocity tracking error at time instant t_k.

3. Finite-time stability of discrete-time systems

The following result is a basic result on finite-time stability and convergence for discrete-time systems, and it was first reported in Sanyal (2019) and Hamrah et al. (2019).

Lemma 3.1: *Consider a discrete-time system with inputs $u_k \in \mathbb{R}^m$ and outputs $y_k \in \mathbb{R}^l$. Define a corresponding positive definite (Lyapunov) function $V : \mathbb{R}^l \to \mathbb{R}$ and let $V_k = V(y_k)$. Let α be a constant as $0 < \alpha < 1$, $\eta \in \mathbb{R}^+$ a constant, and let $\gamma_k := \gamma(V_k)$ where $\gamma : \mathbb{R}_0^+ \to \mathbb{R}_0^+$ is a positive definite function of V_k. Let γ_k satisfy the condition:*

$$\gamma_k \geq \eta \quad \text{for all } V_k \geq \varepsilon, \tag{19}$$

for some (possibly small) constant $\varepsilon \in \mathbb{R}^+$. Then, if V_k satisfies the relation

$$V_{k+1} - V_k \leq -\gamma_k V_k^{\alpha}, \tag{20}$$

the discrete system is (Lyapunov) stable at $y = 0$ and y_k converges to $y = 0$ for $k > N$, where $N \in \mathbb{S}$ is finite.

Proof: The proof of this lemma is given in Hamrah et al. (2019) and Sanyal (2019), and omitted here for brevity. ■

The following statement presents the conditions under which a discrete-time system is finite-time stable using a Lyapunov function that is quadratic in terms of states.

Lemma 3.2: *Consider the discrete-time system*

$$x_{k+1} = \mathscr{B}(x_k) x_k, \tag{21}$$

where $x_k \in \mathbb{R}^n$ and $\mathscr{B} : \mathbb{R}^n \to \mathbb{R}$ is a $\mathcal{C}^o$ function. Define $V_k := V(x_k)$ as follows:

$$V_k := V(x_k) = x_k^{\mathrm{T}} P x_k, \quad P = P^{\mathrm{T}} > 0. \tag{22}$$

and denote $\mathscr{B}_k := \mathscr{B}(x_k)$. The system (21) is finite-time stable under following conditions:

$$\begin{cases} \mathscr{B}_k^2 \leq 1 - \dfrac{\gamma_k}{V_k^{1-\alpha}}, \\ V_k \geq \epsilon = \eta^{\frac{1}{1-\alpha}}, \end{cases} \tag{23}$$

where V_k, γ_k, and η are as defined in Lemma 3.1.

Proof: Evaluating the first finite difference of V_k, one obtains

$$\begin{aligned} V_k^{(1)} := V_{k+1} - V_k &= (x_{k+1} - x_k)^{\mathrm{T}} P (x_k + x_{k+1}) \\ &= x_k^{\mathrm{T}} (\mathscr{B}_k + 1) P (\mathscr{B}_k - 1) x_k \\ &= (\mathscr{B}_k^2 - 1) x_k^{\mathrm{T}} P x_k \\ &= (\mathscr{B}_k^2 - 1) V_k. \end{aligned} \tag{24}$$

According to Lemma 3.1, finite-time stability of system (21) requires that

$$V_{k+1} - V_k \leq -\gamma_k V_k^{\alpha} \quad \text{for } 0 < \alpha < 1,$$

where γ_k is defined as in Lemma 3.1 and satisfies the condition (19). From (20) and (24), we have

$$\begin{aligned} V_{k+1} - V_k \leq -\gamma_k V_k^{\alpha} &\Leftrightarrow (\mathscr{B}_k^2 - 1) V_k \leq -\gamma_k V_k^{\alpha} \\ &\Leftrightarrow \mathscr{B}_k^2 \leq 1 - \frac{\gamma_k}{V_k^{1-\alpha}}. \end{aligned} \tag{25}$$

Noting that $\mathscr{B}^2 \geq 0$, we conclude from (25) that

$$V_k^{1-\alpha} \geq \gamma_k = \gamma(V_k). \tag{26}$$

It is also clear from above that if inequality (26) is reversed, i.e. if $\gamma_k \geq V_k^{1-\alpha}$ for finite k, then that would lead to a contradiction of (25) whereby $\mathscr{B}_k^2 \leq 0$, which can only happen if $\mathscr{B}_k = 0$. This, in turn, would result in finite-time stability of system (21) as $x_{k+1} = \mathscr{B}_k x_k = 0$. This leads us to the conclusion that if γ_k satisfies condition (19) in Lemma 3.1, then system (21) will be finite-time stable. ■

Note that inequality (25) can be used to design $\mathscr{B}_k$ if, for example, it is evaluated as an equality with a $\gamma_k = \gamma(V_k)$ designed to meet the above requirement. In fact, $\gamma(\cdot)$ can be

positive definite function (not-necessary class-$\mathcal{K}$) that meets this requirement, i.e. $\gamma_k \geq \eta$ for all $V_k \geq \eta^{\frac{1}{1-\alpha}}$, $\eta > 0$. Following lemma presents a design for γ which satisfies the conditions given in (23).

Lemma 3.3: *Consider the conditions* (23)*, under which the system* (21) *is shown that is finite-time stable. One possible design for* γ_k *and* $\mathscr{B}_k$ *as a function of* V_k *can be as*

$$\gamma_k = 4c\left(\frac{V_k^{1-\alpha}}{V_k^{1-\alpha}+c}\right)^2 \tag{27}$$

and

$$\mathscr{B}_k = \frac{V_k^{1-\alpha}-c}{V_k^{1-\alpha}+c}, \tag{28}$$

where $c \geq 0$ *is a constant, and* γ_k *and* $\mathscr{B}_k$ *satisfy both conditions in* (23).

Proof: Consider

$$\gamma_k = f(V_k).\left(\frac{V_k^{1-\alpha}}{V_k^{1-\alpha}+c}\right)^2, \tag{29}$$

where $f(V_k)$ is a positive and bounded function. Then, to satisfy the condition (26), it is required to have

$$V_k^{1-\alpha} \geq f(V_k).\left(\frac{V_k^{1-\alpha}}{V_k^{1-\alpha}+c}\right)^2. \tag{30}$$

One can find $f(V_k)$ such that above inequality as well as (25) hold for the designed γ_k, and then the best expression for $\mathscr{B}_k$ will be determined accordingly.

Substituting (29) into (25), one finds

$$\begin{aligned}\mathscr{B}_k^2 &\leq 1 - f(V_k).\frac{V_k^{1-\alpha}}{(V_k^{1-\alpha}+c)^2}\\ &\leq \frac{(V_k^{1-\alpha}+c)^2 - f(V_k).V_k^{1-\alpha}}{(V_k^{1-\alpha}+c)^2}\\ &\leq \frac{(V_k^{1-\alpha})^2 + 2c\,V_k^{1-\alpha} - f(V_k).V_k^{1-\alpha} + c^2}{(V_k^{1-\alpha}+c)^2}.\end{aligned} \tag{31}$$

As noted in Lemma 3.2, $\mathscr{B}^2 \geq 0$ leads to $V_k^{1-\alpha} \geq \gamma_k$, and satisfies the condition (29). Therefore, for $\mathscr{B}^2 \geq 0$, it is required to have

$$\big(f(V_k) - 2c\big)V_k^{1-\alpha} \leq (V_k^{1-\alpha})^2 + c^2. \tag{32}$$

One solution to the above inequality is

$$\big(f(V_k) - 2c\big)V_k^{1-\alpha} = \pm 2c\,V_k^{1-\alpha}, \tag{33}$$

which gives $f(V_k) = 0, 4c$. Since γ_k is a positive definite function by definition, $f(V_k) = 4c$ would be the acceptable answer. Therefore, one obtains expressions for γ_k and $\mathscr{B}_k$ as

$$\begin{cases}\gamma_k = 4c\left(\dfrac{V_k^{1-\alpha}}{V_k^{1-\alpha}+c}\right)^2,\\ \mathscr{B}_k = \dfrac{V_k^{1-\alpha}-c}{V_k^{1-\alpha}+c},\end{cases} \tag{34}$$

which satisfy the conditions given in (23) and guarantee the stability of the system (21). ■

4. Discrete-time stable position tracking control

Defining the discrete-time Lyapunov function quadratic in position tracking error as

$$V(\tilde{b}_k) = V_k = \frac{1}{2}\tilde{b}_k^{\mathrm{T}} P \tilde{b}_k, \tag{35}$$

where $P = P^{\mathrm{T}} \in \mathbb{R}^{3\times 3}$ is a positive definite control gain matrix. The total time difference of this discrete Lyapunov function in the time interval $[t_k, t_{k+1}]$ for $k = 0, 1, \ldots, N$ is then obtained as

$$\begin{aligned}\Delta V_k &= V_{k+1} - V_k = \frac{1}{2}\tilde{b}_{k+1}^{\mathrm{T}} P \tilde{b}_{k+1} - \frac{1}{2}\tilde{b}_k^{\mathrm{T}} P \tilde{b}_k\\ &= \frac{1}{2}(\tilde{b}_{k+1} - \tilde{b}_k)^{\mathrm{T}} P (\tilde{b}_k + \tilde{b}_{k+1}).\end{aligned} \tag{36}$$

A constructive method to obtain FTS position tracking control scheme in discrete time is provided here, which has two steps. In the first step, we develop a discrete vector-valued function of the position and velocity tracking errors that ensures that when this function converges to zero, the errors converge to zero as well. The following statement presents the first step of this method.

Lemma 4.1: *Define* $l(\tilde{b}_k, \tilde{v}_k)$ *as*

$$l(\tilde{b}_k, \tilde{v}_k) := \tilde{v}_k \Delta t + \frac{\beta(\tilde{b}_{k+1} + \tilde{b}_k)}{(\tilde{b}_k^{\mathrm{T}} P \tilde{b}_k)^{1-1/p}}, \tag{37}$$

for the dynamics given in (15)*, where* $\beta > 0$*,* $1 < p < 2$ *and* $\tilde{v}_k = (\tilde{b}_{k+1} - \tilde{b}_k)/\Delta t$*. Let*

$$\begin{aligned}&\tilde{b}_{k+1} = \mathcal{B}(\tilde{b}_k)\tilde{b}_k, \quad \textit{where}\\ &\mathcal{B}(\tilde{b}_k) := \frac{(\tilde{b}_k^{\mathrm{T}} P \tilde{b}_k)^{1-1/p} - \beta}{(\tilde{b}_k^{\mathrm{T}} P \tilde{b}_k)^{1-1/p} + \beta}.\end{aligned} \tag{38}$$

Then the tracking errors $(\tilde{b}_k, \tilde{v}_k)$ *converge to zero in finite time when* $l(\tilde{b}_k, \tilde{v}_k) = 0$*.*

Proof: One can rewrite (38) as

$$\tilde{b}_{k+1} = \tilde{b}_k \frac{(\tilde{b}_k^{\mathrm{T}} P \tilde{b}_k)^{1-1/p} - \beta}{(\tilde{b}_k^{\mathrm{T}} P \tilde{b}_k)^{1-1/p} + \beta}. \tag{39}$$

Hence, it can be simplified to

$$\tilde{b}_{k+1} - \tilde{b}_k = -\frac{\beta(\tilde{b}_{k+1} + \tilde{b}_k)}{(\tilde{b}_k^{\mathrm{T}} P \tilde{b}_k)^{1-1/p}}. \tag{40}$$

Note that this can be re-expressed as

$$-\frac{\beta(\tilde{b}_{k+1}+\tilde{b}_k)}{(\tilde{b}_k^{\mathrm{T}}P\tilde{b}_k)^{1-1/p}}=\tilde{v}_k\Delta t, \tag{41}$$

which holds when $l(\tilde{b}_k,\tilde{v}_k)=0$.

Consider the discrete-time Lyapunov function V_k defined by (35). The difference between the values of this function at successive discrete instants is given by (36). From (40), substituting $\tilde{b}_{k+1}-\tilde{b}_k$ into (36), one gets

$$V_{k+1}-V_k=-\frac{\beta}{2}\frac{(\tilde{b}_{k+1}+\tilde{b}_k)^{\mathrm{T}}P(\tilde{b}_{k+1}+\tilde{b}_k)}{(\tilde{b}_k^{\mathrm{T}}P\tilde{b}_k)^{1-1/p}}. \tag{42}$$

Note that $\tilde{b}_{k+1}+\tilde{b}_k=(1+\mathscr{B}(\tilde{b}_k))\tilde{b}_k$, and the right side of expression (42) is zero if only if

$$\tilde{b}_{k+1}=-\tilde{b}_k,$$

which is possible if and only if $\mathcal{B}(\tilde{b}_k)=-1$ according to (38). From the expression for $\mathscr{B}(\tilde{b}_k)$ in (38), one can see that $\mathcal{B}(\tilde{b}_k)=-1$ if and only if $\tilde{b}_k=0$. Therefore, we conclude that

$$V_{k+1}-V_k=0\Leftrightarrow\tilde{b}_k=0.$$

Now substituting (39) into (42) and noting that $\tilde{b}_k^{\mathrm{T}}P\tilde{b}_k=2V_k$, one obtains

$$V_{k+1}-V_k=-\gamma_k(V_k)^{1/p}, \tag{43}$$

where

$$\gamma_k=4\beta\frac{2^{1-1/p}(V_k)^{2-2/p}}{\left((2V_k)^{1-1/p}+\beta\right)^2}. \tag{44}$$

Clearly, γ_k as given by Equation (44) is a class-$\mathcal{K}$ function of V_k. From Equations (43) and (44), one can see that V_k is monotonously decreasing if $\gamma_k>0$ and

$$0<\gamma_k<\frac{4\beta}{2^{1-1/p}}\quad\text{for } 0<2V_k<\infty.$$

Therefore, γ_k would lead to finite-time stability of the tracking control system. Also from (44), one obtains the ratio:

$$a_k:=\frac{\gamma_k}{\gamma_0}=\frac{(V_k)^{2-2/p}}{(V_0)^{2-2/p}}\frac{\left((2V_0)^{1-1/p}+\beta\right)^2}{\left((2V_k)^{1-1/p}+\beta\right)^2}. \tag{45}$$

This ratio in Equation (45) is bounded below by a positive number in the open interval $(0,1)$ for non-zero V_k and V_0. This guarantees the existence of $\varepsilon\in(0,1)$ and $0<\chi<(V_0)^{1-1/p}$ that satisfy the condition (19) in the statement of Lemma 3.1 for V_k. Therefore, (43) guarantees that V_k converges to zero for $k>N$ for some finite $N\in\mathbb{N}$, and this ensures the finite-time stable convergence of tracking errors to zero. ■

In the second step of finding the FTS position tracking scheme in discrete time, one can create a control force for the error dynamics given in (15) that ensures convergence of the function $l(\tilde{b}_k,\tilde{v}_k)$ derived in the first step to zero in finite time. This will, in turn, ensure that $(\tilde{b}_k,\tilde{v}_k)$ converges to $(0,0)$ in finite time. In order to fulfill this objective, a positive definite Lyapunov function in terms of the obtained vector-valued $l(\tilde{b}_k,\tilde{v}_k)$ is constructed as

$$\mathscr{V}(\tilde{b}_k,\tilde{v}_k)=\frac{1}{2}l(\tilde{b}_k,\tilde{v}_k)^{\mathrm{T}}l(\tilde{b}_k,\tilde{v}_k), \tag{46}$$

which can be used to obtain the FTS tracking control scheme in discrete time. The following statement provides the main result on a finite-time stable position tracking control scheme.

Theorem 4.2: *Consider the translational kinematics and dynamics given by* (15). *Then, the discrete-time force control law given by*

$$\begin{aligned}\bar{\varphi}_k=&\,m\big(v_k+\Delta t\,g\,e_3-\tilde{v}_{k+1}^d\big)\\&-\frac{m}{\Delta t}\left[\left(1+\frac{\kappa}{(l_k^{\mathrm{T}}l_k)^{1-1/p}}\right)\left(1+\frac{\beta}{(\tilde{b}_{k+1}^{\mathrm{T}}P\tilde{b}_{k+1})^{1-1/p}}\right)\right]^{-1}\\&\cdot\left\{\left(1-\frac{\kappa}{(l_k^{\mathrm{T}}l_k)^{1-1/p}}\right)\tilde{v}_k\Delta t\right.\\&-\frac{2\beta}{(\tilde{b}_{k+1}^{\mathrm{T}}P\tilde{b}_{k+1})^{1-1/p}}\left(1+\frac{\kappa}{(l_k^{\mathrm{T}}l_k)^{1-1/p}}\right)\tilde{b}_{k+1}\\&\left.+\frac{\beta(\tilde{b}_{k+1}+\tilde{b}_k)}{(\tilde{b}_k^{\mathrm{T}}P\tilde{b}_k)^{1-1/p}}\left(1-\frac{\kappa}{(l_k^{\mathrm{T}}l_k)^{1-1/p}}\right)\right\},\end{aligned} \tag{47}$$

where $\kappa>0$, and p and β are as defined in Lemma 4.1, *stabilises the translational error dynamics in finite time.*

Proof: Consider the Lyapunov function (46) quadratic in $l(\tilde{b}_k,\tilde{v}_k)$ as constructed in (37). Therefore, the time difference of this discrete-time Lyapunov function can be evaluated as follows:

$$\mathscr{V}_{k+1}-\mathscr{V}_k=\frac{1}{2}(l_{k+1}+l_k)^{\mathrm{T}}(l_{k+1}-l_k). \tag{48}$$

Similar to the definition for $\tilde{b}_{k+1}$ in Lemma 4.1, one can consider

$$l_{k+1}=\mathcal{L}(\tilde{b}_k,\tilde{v}_k)l_k, \tag{49}$$

where

$$\mathcal{L}(\tilde{b}_k,\tilde{v}_k)=\frac{(l_k^{\mathrm{T}}l_k)^{1-1/p}-\kappa}{(l_k^{\mathrm{T}}l_k)^{1-1/p}+\kappa}. \tag{50}$$

Substituting (50) in (49) gives

$$(l_{k+1}-l_k)=-\frac{\kappa}{(l_k^{\mathrm{T}}l_k)^{1-1/p}}(l_{k+1}+l_k). \tag{51}$$

Then according to Lemma 4.1, one can prove similarly that

$$\mathscr{V}_{k+1}-\mathscr{V}_k=-\lambda_k\mathscr{V}_k^{1/p}, \tag{52}$$

where

$$\lambda_k = 4\kappa \frac{2^{1-1/p}(\mathscr{V}_k)^{2-2/p}}{\left((2\mathscr{V}_k)^{1-1/p}+\kappa\right)^2} \tag{53}$$

is a class-$\mathcal{K}$ function of $\mathcal{V}_k$. Also, from (52) and (53), one can see that

$$0 < \lambda_k < \frac{4\kappa}{2^{1-1/p}} \quad \text{for } 0 < 2\mathscr{V}_k < \infty.$$

Therefore, λ_k would lead to finite-time stability of tracking control system.

Now, by substituting $l(\tilde{b}_k, \tilde{v}_k)$ given in (37) into (51), one can obtain

$$\begin{aligned}(\tilde{v}_{k+1}-\tilde{v}_k)\Delta t + \beta\left[\frac{(\tilde{b}_{k+2}+\tilde{b}_{k+1})}{(\tilde{b}_{k+1}^{\mathrm{T}}P\tilde{b}_{k+1})^{1-1/p}} - \frac{(\tilde{b}_{k+1}+\tilde{b}_k)}{(\tilde{b}_k^{\mathrm{T}}P\tilde{b}_k)^{1-1/p}}\right] \\ = -\frac{\kappa}{(l_k^{\mathrm{T}}l_k)^{1-1/p}}\left\{(\tilde{v}_{k+1}+\tilde{v}_k)\Delta t \right. \\ \left. + \beta\left[\frac{(\tilde{b}_{k+2}+\tilde{b}_{k+1})}{(\tilde{b}_{k+1}^{\mathrm{T}}P\tilde{b}_{k+1})^{1-1/p}} + \frac{(\tilde{b}_{k+1}+\tilde{b}_k)}{(\tilde{b}_k^{\mathrm{T}}P\tilde{b}_k)^{1-1/p}}\right]\right\}. \end{aligned} \tag{54}$$

Noting that $(\tilde{b}_{k+2}-\tilde{b}_{k+1})/\Delta t = \tilde{v}_{k+1}$, one can solve above expression for $\tilde{v}_{k+1}$ to obtain the discrete-time translational error dynamics equation as

$$\begin{aligned}\tilde{v}_{k+1} &= \mathcal{F}(\tilde{b}_k, \tilde{b}_{k+1}, \tilde{v}_k, l_k) \\ &= \frac{1}{\Delta t}\left[\left(1+\frac{\kappa}{(l_k^{\mathrm{T}}l_k)^{1-1/p}}\right)\left(1+\frac{\beta}{(\tilde{b}_{k+1}^{\mathrm{T}}P\tilde{b}_{k+1})^{1-1/p}}\right)\right]^{-1} \\ &\quad \cdot\left\{\left(1-\frac{\kappa}{(l_k^{\mathrm{T}}l_k)^{1-1/p}}\right)\tilde{v}_k\Delta t \right. \\ &\quad -\frac{2\beta}{(\tilde{b}_{k+1}^{\mathrm{T}}P\tilde{b}_{k+1})^{1-1/p}}\left(1+\frac{\kappa}{(l_k^{\mathrm{T}}l_k)^{1-1/p}}\right)\tilde{b}_{k+1} \\ &\quad \left.+\frac{\beta(\tilde{b}_{k+1}+\tilde{b}_k)}{(\tilde{b}_k^{\mathrm{T}}P\tilde{b}_k)^{1-1/p}}\left(1-\frac{\kappa}{(l_k^{\mathrm{T}}l_k)^{1-1/p}}\right)\right\}, \end{aligned} \tag{55}$$

Then, noting that $\tilde{v}_{k+1} = v_{k+1} - v_{k+1}^d$, one can obtain the discrete-time control force vector given by (47) after substituting (55) in the second equation of (15). The discrete-time control force vector so obtained, guarantees the finite-time stability of the position tracking control. ■

The following section provides a finite-time stable feedback control law in discrete-time to stabilise the attitude error dynamics (15).

5. Discrete finite-time stable attitude tracking control

In this section, a finite-time stable attitude tracking control scheme in discrete time is provided. The following two lemmas are also used to prove the main result.

Lemma 5.1: *Let x and y be non-negative real numbers and let p as defined in* 4.1. *Then*

$$x^{(1/p)} + y^{(1/p)} \geq (x+y)^{(1/p)}. \tag{56}$$

Moreover, the above inequality is a strict inequality if both x and y are non-zero.

Lemma 5.2: *Let $K = \mathrm{diag}(k_1, k_2, k_3)$, where $k_1 > k_2 > k_3 \geq 1$. Define*

$$s_K(Q) = \sum_{i=1}^{3} k_i (Q^{\mathrm{T}} e_i) \times e_i, \tag{57}$$

such that $\frac{\mathrm{d}}{\mathrm{d}t}\langle K, I-Q\rangle = \omega^{\mathrm{T}} s_K(Q)$. Here, $\langle A, B\rangle = \mathrm{tr}(A^{\mathrm{T}}B)$, which makes $\langle K, I-Q\rangle$ a Morse function defined on SO(3). *Let $\mathcal{S} \subset$ SO(3) be a closed subset containing the identity in its interior, defined by*

$$\begin{aligned}\mathcal{S} = \big\{&Q \in \mathrm{SO}(3) : Q_{ii} \\ &\geq 0 \text{ and } Q_{ij}Q_{ji} \leq 0 \;\forall\, i, j \in \{1,2,3\},\; i \neq j\big\}. \end{aligned} \tag{58}$$

Then for $Q \in \mathcal{S}$, we have

$$s_K(Q)^T s_K(Q) \geq \mathrm{tr}(K - KQ). \tag{59}$$

Proof: The proof of this lemma is given in Bohn and Sanyal (2015), and omitted here for brevity. ■

The discrete finite-time attitude tracking control scheme and its proof of stability and domain of convergence are given as follows.

Theorem 5.3: *Consider the discretised rotational error kinematics and the real dynamics of an underactuated vehicle given in* (15), *with $s_K(Q_k)$ as defined in* (57). *Define*

$$z_K(Q_k) = \frac{s_K(Q_k)}{\left(s_K^{\mathrm{T}}(Q_k)s_K(Q_k)\right)^{1-1/p}}, \tag{60}$$

where p is as defined in Lemma 5.1, *and let k_l be a constant in the interval* (0, 1]. *Then, the discrete-time control law given by*

$$\begin{aligned}u_k = J\Bigg(&\left[\frac{(\psi_k^{\mathrm{T}}J\psi_k)^{1-1/p}-\Gamma}{(\psi_k^{\mathrm{T}}J\psi_k)^{1-1/p}+\Gamma}\right](\omega_k + k_l z_K(Q_k)) \\ &- k_l z_K(Q_{k+1}) + Q_{k+1}^{\mathrm{T}}\Omega_{k+1}^d\Bigg) - F_k^{\mathrm{T}} J\Omega_k, \end{aligned} \tag{61}$$

stabilises the rotational error dynamics

$$\omega_{k+1} = \left[\frac{(\psi_k^{\mathrm{T}}J\psi_k)^{1-1/p}-\Gamma}{(\psi_k^{\mathrm{T}}J\psi_k)^{1-1/p}+\Gamma}\right]\psi_k(\omega_k, Q_k) - k_l z_K(Q_{k+1}) \tag{62}$$

in finite time, where $\psi_k(\omega_k, Q_k)$ is defined as

$$\psi_k(\omega_k, Q_k) = \omega_k + k_l z_K(Q_k). \tag{63}$$

Proof: Consider $\omega_k = -k_l z_K(Q_k)$ and discretised error kinematics given in (15) and define the discrete-time Morse function $U_k = k_p\langle I - Q_k, K\rangle$ on SO(3) where $k_p > 1$. Then the first time difference of this discrete-time Morse function along the attitude kinematics is given by

$$\begin{aligned} U_{k+1} - U_k &= k_p \left\langle Q_k - Q_{k+1}, K \right\rangle \\ &= k_p \langle -Q_k \varpi_k^{\times}, K\rangle \\ &= k_p \langle \varpi_k^{\times}, -Q_k^{\mathrm{T}} K\rangle \\ &= \frac{1}{2} k_p \langle \varpi_k^{\times}, KQ_k - Q_k^{\mathrm{T}} K\rangle \\ &= k_p \varpi_k^{\mathrm{T}} S_K(Q_k). \end{aligned} \tag{64}$$

Substituting $\varpi_k = \Delta t\, \omega_k$ in (64), one finds

$$\begin{aligned} k_p \varpi_k^{\mathrm{T}} S_K(Q_k) &= -\Delta t\, k_p\, k_l\, z_K(Q_k)^{\mathrm{T}} s_K(Q_k) \\ &= -k_p\, k_l\, \Delta t \big(s_K(Q_k)^{\mathrm{T}} s_K(Q_k)\big)^{1/p} \\ &\le -k_p\, k_l\, \Delta t \big(\langle I - Q_k, K\rangle \big)^{1/p} \\ &\le -k_l\, \Delta t \big(k_p\, \langle I - Q_k, K\rangle \big)^{1/p}, \end{aligned} \tag{65}$$

where we employed inequality (59) in Lemma 5.2. Therefore, when $\psi_k = 0$, one can conclude that $\langle I - Q_k, K\rangle \to 0$ in finite time for all initial Q_k in the subset $\mathcal{S} \subset \mathrm{SO}(3)$ defined in Lemma 5.1, which yields $Q_k \to I$ in finite time once $Q_k \in \mathcal{S}$. Moreover, as $\Delta U_k = U_{k+1} - U_k$ is negative definite when $\psi_k = 0$, it keeps decreasing in time and therefore Q_k will reach $\mathcal{S}$ in finite time. Therefore, $Q_k \to I$ in finite time.

The control law is then designed to ensure that $\psi_k(\omega_k, Q_k) \to 0$ in finite time. Define the Morse–Lyapunov function

$$\mathcal{V}_k(\omega_k, Q_k) = \frac{1}{2} \psi_k(\omega_k, Q_k)^{\mathrm{T}} \psi_k(\omega_k, Q_k) + k_p\, \langle I - Q_k, K\rangle\,. \tag{66}$$

The time difference of this discrete-time Morse–Lyapunov function can be evaluated as follows:

$$\begin{aligned} \mathcal{V}_{k+1} - \mathcal{V}_k &= \frac{1}{2} \psi_{k+1}^{\mathrm{T}} J \psi_{k+1} - \frac{1}{2} \psi_k^{\mathrm{T}} J \psi_k + k_p \left\langle Q_k - Q_{k+1}, K \right\rangle \\ &= \frac{1}{2} (\psi_{k+1} + \psi_k)^{\mathrm{T}} J (\psi_{k+1} - \psi_k) \\ &\quad + k_p \left\langle Q_k - Q_{k+1}, K \right\rangle. \end{aligned} \tag{67}$$

One can consider

$$\psi_{k+1} = \Psi(\omega_k, Q_k) \psi_k, \tag{68}$$

where

$$\Psi(\omega_k, Q_k) = \frac{(\psi_k^{\mathrm{T}} J \psi_k)^{1-1/p} - \Gamma}{(\psi_k^{\mathrm{T}} J \psi_k)^{1-1/p} + \Gamma}, \tag{69}$$

and let $\Gamma > 0$.

Substituting (69) in (68) gives

$$(\psi_{k+1} - \psi_k) = -\frac{\Gamma}{(\psi_k^{\mathrm{T}} J \psi_k)^{1-1/p}} (\psi_{k+1} + \psi_k). \tag{70}$$

Therefore, one can rewrite (67) as

$$\begin{aligned} \mathcal{V}_{k+1} - \mathcal{V}_k = &-\frac{\Gamma}{2} \frac{(\psi_{k+1} + \psi_k)^{\mathrm{T}} J (\psi_{k+1} + \psi_k)}{(\psi_k^{\mathrm{T}} J \psi_k)^{1-1/p}} \\ &+ k_p\, \varpi_k^{\mathrm{T}} S_K(Q_k). \end{aligned} \tag{71}$$

Note that the first term on the right-hand side of expression (71) is zero if and only if

$$\psi_{k+1} = -\psi_k,$$

which is possible if and only if $\Psi(\omega_k, Q_k) = -1$ according to (68). From (69), one can see that $\Psi(\omega_k, Q_k) = -1$ if and only if $\psi_k = 0$. Therefore, from (68) and (69) we conclude that

$$-\frac{\Gamma}{2} \frac{(\psi_{k+1} + \psi_k)^{\mathrm{T}} J (\psi_{k+1} + \psi_k)}{(\psi_k^{\mathrm{T}} J \psi_k)^{1-1/p}} = 0 \Leftrightarrow \psi_k = 0.$$

Therefore, the first term on the right-hand side of expression (71) can be simplified as follows:

$$-\frac{\Gamma}{2} \frac{(\psi_{k+1} + \psi_k)^{\mathrm{T}} J (\psi_{k+1} + \psi_k)}{(\psi_k^{\mathrm{T}} J \psi_k)^{1-1/p}} = -\rho_k (\psi_k^{\mathrm{T}} J \psi_k)^{1/p}, \tag{72}$$

where

$$\rho_k = 4\Gamma \frac{(0.5)^{1-1/p} (\psi_k^{\mathrm{T}} J \psi_k)^{2-2/p}}{\big((\psi_k^{\mathrm{T}} J \psi_k)^{1-1/p} + \Gamma\big)^2}. \tag{73}$$

From Equations (72) and (73), one can see that the first term on the right-hand side of expression (71) is monotonously decreasing if

$$0 < \rho_k < \frac{4\Gamma}{2^{1-1/p}} \quad \text{for } 0 < \psi_k^{\mathrm{T}} J \psi_k < \infty.$$

Therefore, using (65) and (72), the expression (71) is evaluated as follows:

$$\begin{aligned} \Delta \mathcal{V}_k &= -\rho_k (\psi_k^{\mathrm{T}} J \psi_k)^{1/p} - k_p k_l \Delta t \big(s_K(Q_k)^{\mathrm{T}} s_K(Q_k)\big)^{1/p} \\ &\le -(\psi_k^{\mathrm{T}} J \psi_k)^{1/p} - k_l\, \Delta t \big(k_p\, \langle I - Q_k, K\rangle \big)^{1/p} \\ &\le -k_l\, \Delta t \Big((\psi_k^{\mathrm{T}} J \psi_k)^{1/p} + \big(k_p\, \langle I - Q_k, K\rangle \big)^{1/p} \Big). \end{aligned} \tag{74}$$

for $(Q_k, \omega_k) \in \mathcal{S} \times \mathbb{R}^3$. Finally, using inequality (56) in Lemma 5.1, one obtains

$$\begin{aligned} \Delta \mathcal{V}_k &\le -k_l\, \Delta t \Big(\psi_k^{\mathrm{T}} J \psi_k + k_p\, \langle I - Q_k, K\rangle \Big)^{1/p} \\ &\le -k_l\, \Delta t\, \mathcal{V}_k^{1/p}, \end{aligned} \tag{75}$$

where $k_p > 0$, and $0 < k_l \le 1$. Therefore, all initial states of the feedback attitude system, which start in the domain of attraction of the equilibrium $(I, 0)$ and for which the value of the Lyapunov

function $\mathcal{V}$ is finite, converge to $(I,0)$ in finite time. Now, by substituting $\psi_k(\omega_k, Q_k)$ given in (63) into (68), one can obtain

$$\omega_{k+1} = \Psi(\omega_k, Q_k)\big(\omega_k + k_l z_K(Q_k)\big) - k_l z_K(Q_{k+1}) \tag{76}$$

or

$$\omega_{k+1} = \left[\frac{(\psi_k^{\mathrm{T}} J \psi_k)^{1-1/p} - \Gamma}{(\psi_k^{\mathrm{T}} J \psi_k)^{1-1/p} + \Gamma}\right] \psi_k(\omega_k, Q_k) - k_l z_K(Q_{k+1}). \tag{77}$$

From the discretised dynamics equation of rotational motion obtained in the form of a LGVI given in (15) as

$$J\,\Omega_{k+1} = F_k^{\mathrm{T}} J \Omega_k + u_k, \tag{78}$$

where

$$\Omega_{k+1} = \omega_{k+1} + Q_{k+1}^{\mathrm{T}} \Omega_{k+1}^d, \tag{79}$$

one can find the discrete-time control law u_k that guarantees the stability of the attitude tracking control in a finite time, as follows:

$$u_k = J\left(\left[\frac{(\psi_k^{\mathrm{T}} J \psi_k)^{1-1/p} - \Gamma}{(\psi_k^{\mathrm{T}} J \psi_k)^{1-1/p} + \Gamma}\right]\big(\omega_k + k_l z_K(Q_k)\big) - k_l z_K(Q_{k+1}) + Q_{k+1}^{\mathrm{T}} \Omega_{k+1}^d\right) - F_k^{\mathrm{T}} J \Omega_k. \tag{80}$$

■

Remark 5.1: **(Almost global domain of attraction of the control scheme):** Analysing the time difference of the Morse–Lyapunov function (66) showed that this function satisfies the sufficient condition for finite-time stability. From prior research on almost global asymptotic attitude stabilisation and tracking in Chaturvedi et al. (2011), Sanyal et al. (2011), and Sanyal and Chaturvedi (2008), we know that the subset of SO(3) where $s_K(Q_k) = 0$, which is also the set of critical points for $\langle I - Q_k, K\rangle$, is

$$C \triangleq \{I,\ \mathrm{diag}(1,-1,-1),\ \mathrm{diag}(-1,1,-1),\ \mathrm{diag}(-1,-1,1)\} \subset \mathrm{SO}(3).$$

Therefore, the subset of the state space where $V_{k+1} - V_k = 0$ is $\{(Q_k, \omega_k) : Q_k \in C \text{ and } \omega_k = 0\} \subset \mathrm{SO}(3) \times \mathbb{R}^3 \simeq \mathrm{TSO}(3)$. This subset is also the set of equilibria for tracking errors in the feedback attitude system, and its largest invariant set. Among the four equilibria in this set, the equilibrium $(Q_k, \omega_k) = (I, 0)$ is attractive as it corresponds to the minimum value of $V_k(Q_k, \omega_k)$. Other three equilibria are unstable equilibria. All trajectories that do not start on the stable manifolds of the other three equilibria converge to the stable equilibrium $(I, 0)$. The Lyapunov function along a state trajectory on any of these stable manifolds increases in value when going backwards in time. A state trajectory on a stable manifold of any of this unstable equilibria cannot approach itself outside of a closed neighbourhood containing the equilibrium. Therefore, the stable manifolds of these unstable equilibria from nowhere dense subsets of $\mathrm{SO}(3) \times \mathbb{R}^3$. Denote the union of these stable manifolds of the unstable equilibria as M. The complement of M is therefore dense and open in $\mathrm{TSO}(3) \simeq \mathrm{SO}(3) \times \mathbb{R}^3$. All initial states that are in the complement $\mathrm{SO}(3) \times \mathbb{R}^3/M$ converge to the stable equilibrium $(I, 0)$, which makes its domain of attraction almost global.

6. Robustness analysis of discrete-time FTS attitude tracking control scheme

The finite-time stability property of the attitude tracking control law given in Theorem 5.3 results in guaranteed convergence of almost any initial attitude state to the desired state, given by the tracking errors $(Q, \omega) = (I, 0)$, in finite time in the absence of any disturbances to the discretised dynamics model. In the presence of a bounded disturbance control input u_k^D in the dynamics, all attitude tracking errors will converge to a bounded neighbourhood of $(I, 0)$ as well. The following result gives a conservative statement relating the bound of tracking errors that can be tolerated and bounds on the neighbourhood of $(I, 0)$.

Corollary 6.1: *Consider the discretised feedback system given by the attitude kinematics and dynamics in the last two equations* (15)*, and the control law* (80)*. Let $\mathcal{N} \subset S \times \mathbb{R}^3$, where S is as defined in Equation* (58)*, be a closed neighbourhood of $(I, 0)$ defined by*

$$\mathcal{N} := \big\{(Q_k, \omega_k) : \|s_K(Q_k)\| \le s_{\max} \text{ and } \|\psi_k\| \le \Psi_{\max} < 1\big\}. \tag{81}$$

If the norm of the disturbance in control input, u_k^D, satisfies the following inequality:

$$\|u_k^D\| \le \frac{k_l\,\Delta t\left(\Psi_{\max}^{(2/p)} + s_{\max}^{(2/p)}\right)}{\Psi_{\max}}, \tag{82}$$

then, the tracking errors (Q, ω) converge to the neighbourhood $\mathcal{N}$ in finite time.

Proof: Consider the discretised attitude dynamics of a rigid body in LGVI form given in (15) disturbed by a control input u_k^D,

$$J\,\Omega_{k+1} = F_k^{\mathrm{T}} J \Omega_k + u_k + u_k^D \tag{83}$$

which has an additional term (u_k^D) due to the disturbance control input, and noting that

$$\omega_{k+1} = \Omega_{k+1} - Q_{k+1}^{\mathrm{T}} \Omega_{k+1}^d$$

and

$$\psi_k(\omega_k, Q_k) = \omega_k + k_l z_K(Q_k),$$

then, we can write

$$\begin{aligned}\psi_{k+1} - \psi_k &= \Omega_{k+1} - Q_{k+1}^{\mathrm{T}} \Omega_{k+1}^d - \Omega_k + Q_k^{\mathrm{T}} \Omega_k^d \\ &\quad + k_l\Big(z_K(Q_{k+1}) - z_K(Q_k)\Big) \\ &= J^{-1} F_k^{\mathrm{T}} J \Omega_k + J^{-1} u_k + J^{-1} u_k^D - Q_{k+1}^{\mathrm{T}} \Omega_{k+1}^d \\ &\quad - \Omega_k + Q_k^{\mathrm{T}} \Omega_k^d + k_l\Big(z_K(Q_{k+1}) - z_K(Q_k)\Big) \\ &= -\frac{\Gamma(\psi_{k+1} + \psi_k)}{(\psi_k^{\mathrm{T}} J \psi_k)^{1-1/p}} + J^{-1} u\end{aligned} \tag{84}$$

Substituting (84) into the time difference of discrete-time Lyapunov function given in (67) and simplifying, we get

$$\begin{aligned}\mathcal{V}_{k+1}-\mathcal{V}_k &= \frac{1}{2}(\psi_{k+1}+\psi_k)^{\mathrm{T}}J\left[-\frac{\Gamma(\psi_{k+1}+\psi_k)}{(\psi_k^{\mathrm{T}}J\psi_k)^{1-1/p}}+J^{-1}u_k^D\right]\\ &\quad + k_p\langle Q_k-Q_{k+1},K\rangle\\ &= -\rho_k(\psi_k^{\mathrm{T}}J\psi_k)^{1/p}-k_p\,k_l\,\Delta t\big(s_K(Q_k)^{\mathrm{T}}s_K(Q_k)\big)^{1/p}\\ &\quad + \frac{1}{2}(\psi_{k+1}+\psi_k)^{\mathrm{T}}u_k^D. \end{aligned} \tag{85}$$

Now, since $\|\psi_{k+1}+\psi_k\| \le \|\psi_{k+1}\|+\|\psi_k\| \le 2\Psi_{max}$, the last term on the right side of the above equation is upper bounded as follows:

$$\frac{1}{2}(\psi_{k+1}+\psi_k)u_k^D \le \frac{1}{2}\|\psi_{k+1}+\psi_k\|\|u_k^D\| \le \Psi_{\max}\|u_k^D\|. \tag{86}$$

From $AB \le \|A\|.\|B\|$, we can rewrite the time difference of Lyapunov function as

$$\begin{aligned}\mathcal{V}_{k+1}-\mathcal{V}_k &\le -\rho_k(\psi_k^{\mathrm{T}}J\psi_k)^{1/p}-k_p\,k_l\,\Delta t\big(\langle I-Q_k,K\rangle\big)^{1/p}\\ &\quad + \frac{1}{2}\|\psi_{k+1}+\psi_k\|\|u_k^D\|\\ &\le -(\psi_k^{\mathrm{T}}J\psi_k)^{1/p}-k_l\,\Delta t\big(k_p\langle I-Q_k,K\rangle\big)^{1/p}\\ &\quad + \frac{1}{2}\|\psi_{k+1}+\psi_k\|\|u_k^D\|\\ &\le -k_l\,\Delta t\Big((\psi_k^{\mathrm{T}}J\psi_k)^{1/p}+\big(k_p\langle I-Q_k,K\rangle\big)^{1/p}\Big)\\ &\quad + \frac{1}{2}\|\psi_{k+1}+\psi_k\|\|u_k^D\|\\ &\le -k_l\,\Delta t\Big(\psi_{\max}^{(1/p)}+s_{\max}^{(1/p)}\Big)+\Psi_{\max}\|u_k^D\|. \end{aligned} \tag{87}$$

Therefore, $\mathcal{V}_{k+1}-\mathcal{V}_k$ is non-positive along the boundary of N if

$$-k_l\,\Delta t\Big(\psi_{\max}^{(1/p)}+s_{\max}^{(1/p)}\Big)+\Psi_{\max}\|u_k^D\| \le 0, \tag{88}$$

which is a sufficient condition for all trajectories starting outside the boundary of neighbourhood $\mathcal{N}$ to converge to this neighbourhood of $(I,0)$. Expression (88) leads to (82) for the bound on the norm of the disturbance u_k^D for which convergence of errors to the neighbourhood $\mathcal{N}$ of $(I,0)$ is guaranteed. ■

Remark 6.1: In the presence of bounded disturbances and internal parametric uncertainties in the dynamics of the rigid body, state trajectories will converge to a bounded neighbourhood of $(Q,\omega)=(I,0)$. On the other hand, based on a desired size of this neighbourhood, one can find an upper bound on the norm of external disturbances and internal parametric uncertainties that can be tolerated for state trajectories to converge to this neighbourhood. This can be done using the Lyapunov analysis presented in the proof of the almost global finite-time stability of the tracking control scheme given in Theorems 4.2 and 5.3.

7. Continuous finite-time stable tracking control on TSE(3)

A FTS tracking control scheme in continuous time has been reported in Prabhakaran, Sanyal, and Warier (2017). In this scheme, the error dynamics in continuous time is given by

$$\begin{cases} m\dot{\tilde{v}} = m\,g\,e_3-\varphi_c-v^d,\\ J\dot{\omega} = \tau_c+J(\omega^{\times}Q^{\mathrm{T}}\Omega^d-Q^{\mathrm{T}}\dot{\Omega}^d)-(\omega+Q^{\mathrm{T}}\Omega^d)^{\times}J(\omega+Q^{\mathrm{T}}\Omega^d), \end{cases} \tag{89}$$

where τ_c and $\varphi_c \in \mathbb{R}^3$ are obtained from the feedback control laws in continuous time as follows:

$$\begin{aligned}\tau_c &= J\left(Q^{\mathrm{T}}\dot{\Omega}^d-\frac{\kappa_r H(s_K(Q))}{\big(s_K^{\mathrm{T}}(Q)s_K(Q)\big)^{1-1/p}}w(Q,\omega)\right)\\ &\quad + (Q^{\mathrm{T}}\Omega^d)^{\times}J\big(Q^{\mathrm{T}}\Omega^d-\kappa_r z_K(Q)\big)+\kappa_r J\big(z_K(Q)\times Q^{\mathrm{T}}\Omega^d\big)\\ &\quad + \kappa_r J(\omega+Q^{\mathrm{T}}\Omega^d)\times z_K(Q)-k_p s_K(Q)\\ &\quad - \frac{L_\Omega\Psi(Q,\omega)}{\big(\Psi(Q,\omega)^{\mathrm{T}}L_\Omega\Psi(Q,\omega)\big)^{1-1/p}} \end{aligned} \tag{90}$$

and

$$\varphi_c = ge_3-\dot{v}_d+\kappa_t(\dot{z}+\tilde{b})+\frac{\kappa_t P_r(\tilde{v}+\kappa_t z)}{\big[(\tilde{v}+\kappa_t z)^{\mathrm{T}}P_r(\tilde{v}+\kappa_t z)\big]^{1-1/p}}. \tag{91}$$

In Equations (90) and (91),

$$\Psi(Q,\omega) = \omega+\kappa z_K(Q), \tag{92}$$

$$H(x) = I-\frac{2(1-1/p)}{x^{\mathrm{T}}x}xx^{\mathrm{T}}, \tag{93}$$

$$z(t) = \frac{\tilde{b}}{(\tilde{b}^{\mathrm{T}}\tilde{b})^{1-1/p}}, \tag{94}$$

$$\dot{z} = \frac{(\tilde{b}^{\mathrm{T}}\tilde{b})^{1-1/p}\tilde{v}-(2-2/p)(\tilde{b}^{\mathrm{T}}\tilde{b})^{-1/p}(\tilde{b}^{\mathrm{T}}\tilde{v})\tilde{b}}{(\tilde{b}^{\mathrm{T}}\tilde{b})^{2-2/p}}, \tag{95}$$

where $P_r \in \mathbb{R}^{3\times3}$ is a positive definite control gain matrix, and p is as defined in Lemma 5.1. Further, L_Ω is a positive definite control gain matrix such that $L_\Omega - J$ is positive semi-definite, $k_p > 1$ and the control gain κ is defined by

$$\kappa^p = \frac{\sigma_{L,\min}}{\sigma_{J,\max}} > 0.$$

These continuous control laws guarantee the finite-time stability of the feedback tracking error dynamics given by (89) at $(Q,\omega,\tilde{b},\tilde{v})=(I,0,0,0)$. These control laws are then sampled over the time interval $[t_0,t_f]$ and with a time step size Δt.

The following section presents numerical results obtained by implementing this paper's proposed FTS scheme in discrete time compared to the results of the sampled continuous-time FTS scheme.

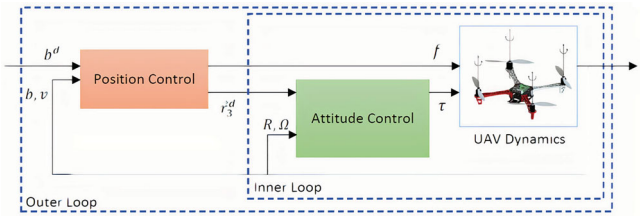

Figure 2. Block diagram of a quadcopter UAV control system.

8. Simulation results

This section presents numerical simulation results for the FTS tracking control scheme in discrete time. These simulation results are provided for a quadcopter UAV with a mass $m = 4$ kg, for time period of $T = 5$ s, and with time step size of $\Delta t = 0.01$ s using discrete-time FTS control laws obtained in (47) and (80). Figure 2 shows the block diagram of a control system for controlling a quadcopter UAV to follow a time-varying desired position, b_k^d. This system has two loops: an inner loop for attitude control and an outer loop for position control. The desired attitude (R_k^d) that is to be tracked, is generated using the desired control force vector given by an outer loop position tracking scheme.

8.1 Numerical simulation results for discrete-time FTS position and attitude tracking control schemes

A helical desired position trajectory with the following initial conditions is used for both control loops:

$$b_k^d = b^d(t_k) = [0.4 \sin \pi t_k \quad 0.6 \cos \pi t_k \quad 0.4\, t_k]^{\mathrm{T}},$$
$$b_0 = [1 \quad 0 \quad 0]^{\mathrm{T}}, \quad v_0 = [0 \quad 0 \quad 0]^{\mathrm{T}},$$
$$R_0 = I, \quad \Omega_0 = [0 \quad 0 \quad 0]^{\mathrm{T}}, \quad \Omega_0^d = [0 \quad 0 \quad 0]^{\mathrm{T}}.$$

The gains are selected after trial and error for the FTS discrete-time attitude tracking scheme as follows:

$$P = 4\,\mathbf{I}_{3\times 3}, \quad \beta = 0.01, \quad \kappa = 0.009,$$
$$k_l = 0.01, \quad \Gamma = 0.1,$$

and for the FTS sampled continuous time scheme as follows:

$$P_r = 5\,\mathbf{I}_{3\times 3}, \quad \kappa_t = 0.8,$$
$$L_\Omega = 3.5\,\mathbf{I}_{3\times 3}, \quad k_p = 4.5, \quad \kappa_r = 0.04,$$

which provide desirable and similar transient response characteristics of both tracking control schemes when $\Delta t = 0.01$. The time trajectory of the UAV tracking the desired trajectory is shown in Figure 3 and it shows that the trajectory converges to the desired values in a finite time stable manner.The results of the numerical simulation for the discrete-time FTS tracking control laws obtained in (47) and (80) for $\Delta t = 0.01$ and $t_f = 5$ s are shown in Figure 4. Figure 4(a,b) show that the translational motion tracking errors converge to zero in finite time. Figure 4(c,d) indicate the finite-time convergence of rotational motion tracking errors to zero. The attitude tracking error is

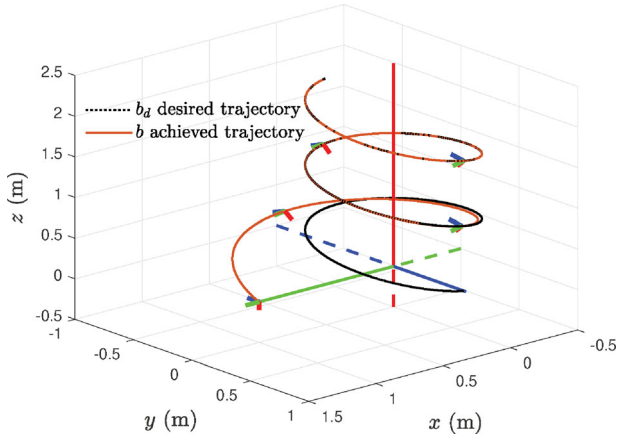

Figure 3. Time trajectory of UAV.

parameterised by the principal rotation angle Φ of the attitude error matrix Q, and is given by

$$\Phi = \cos^{-1}\left(\frac{1}{2}\big(\mathrm{tr}(Q) - 1\big)\right). \tag{96}$$

Convergence of the attitude tracking error Φ in finite time, as shown in Figure 4(d), implies that R tracks the desired trajectory R^d. The time plots of the control inputs f_k and τ_k in Figure 4(e,f), respectively, show that the control effort is within reasonable bounds and practically achievable for multi-rotor UAVs. Therefore, the discrete-time tracking control scheme proposed here is able to track the desired trajectory in finite time.

8.2 Comparison with a sampled continuous-time tracking scheme

The performance of the proposed FTS tracking control scheme in discrete time is compared here to that of the sampled continuous-time FTS tracking scheme presented in Section 7. Result of numerical simulations are provided for the same quadcopter UAV given above but for different time periods of $T = 5$, 25, and 50 s, with different time step sizes of $\Delta t = 0.01, 0.05$, and 0.1 s and the same total number of time steps, using discrete-time FTS control laws obtained in (47) and (80), and the sampled continuous-time control laws given in Prabhakaran, Sanyal, and Warier (2017). Simulation results are presented in Figures 5–9 to compare the performance of the discrete-time FTS tracking scheme with a sampled continuous-time FTS tracking scheme for *different values of the time step size*. From these plots, one can conclude that the control law obtained by sampling the continuous FTS control input does not ensure the stability in tracking when the time step size changes. Moreover, to have a definite result of the comparison between results of these two schemes, a parameter study that was first proposed and used in Hamrah et al. (2019) is used here to confirm how the value of the Lyapunov function behaves at certain time instants. This tests whether the Lyapunov function increases in value between two successive sampling instants, and whether that increase is significant or is just an artifact of machine (float) precision. The results of this comparison are given in Table 1, where $\Delta \mathbb{V}_{\max}$ denotes the maximum positive value of the time

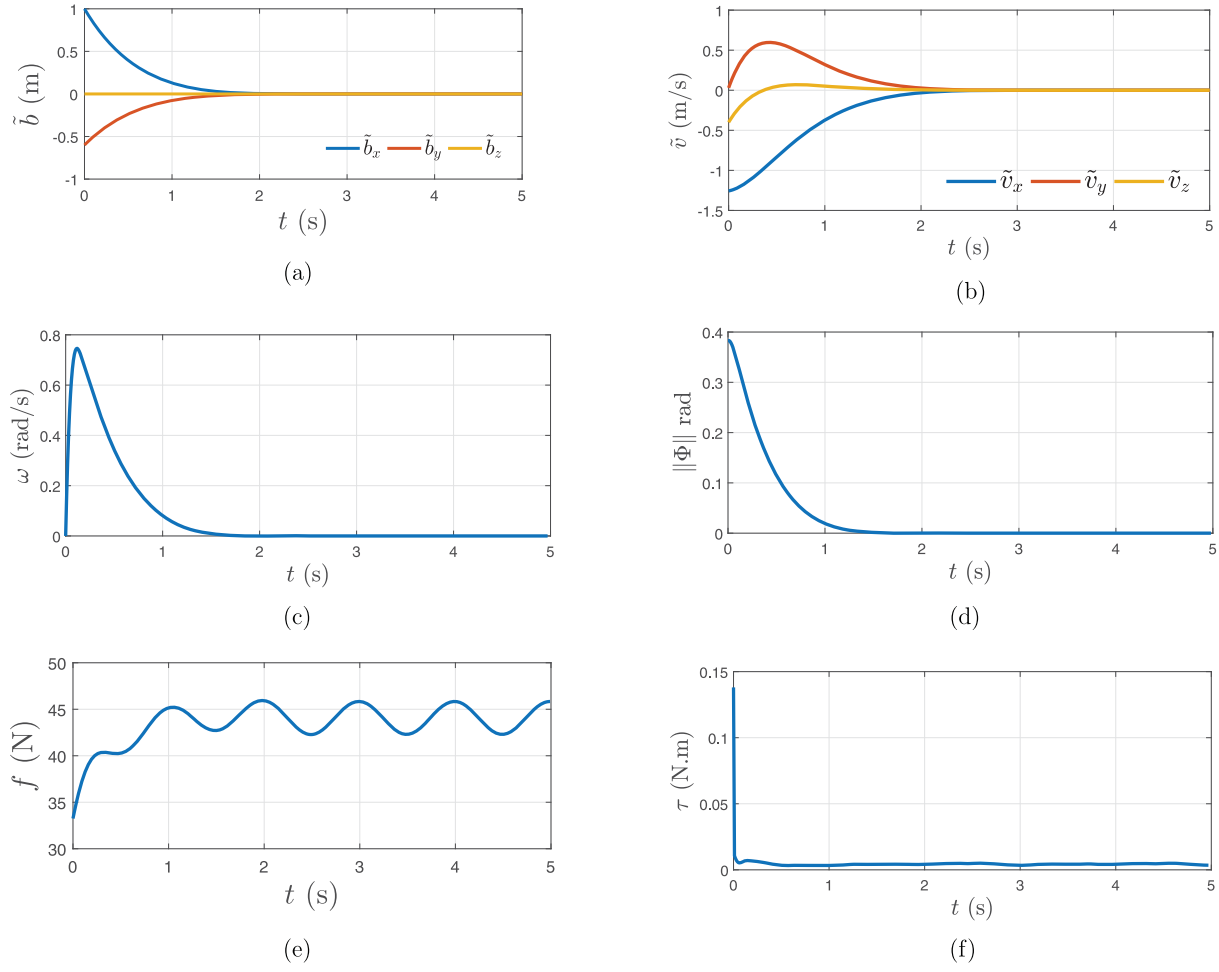

Figure 4. Tracking errors and control laws for discrete-time FTS tracking control scheme for $\Delta t = 0.01$ and $t_f = 5$ s. (a) Position tracking error. (b) Velocity tracking error. (c) Angular velocity error. (d) Attitude tracking error function. (e) Total thrust force. (f) Torque control.

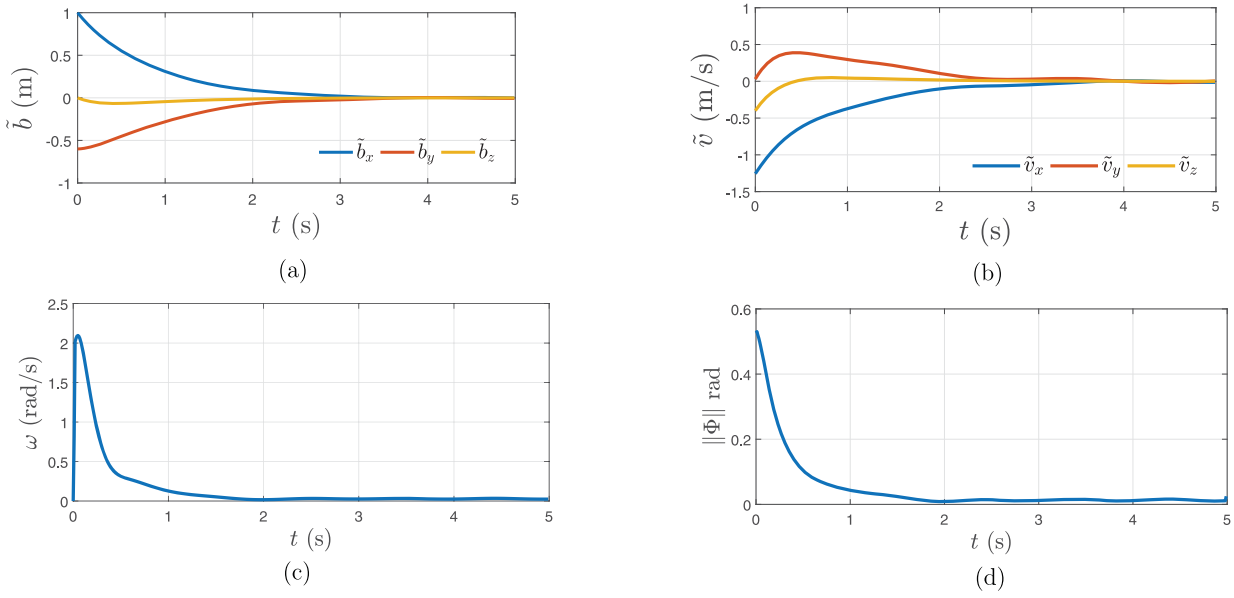

Figure 5. Tracking errors for sampled FTS continuous tracking control scheme for $\Delta t = 0.01$ and $t_f = 5$ s. (a) Position tracking error. (b) Velocity tracking error. (c) Angular velocity error. (d) Attitude tracking error function.

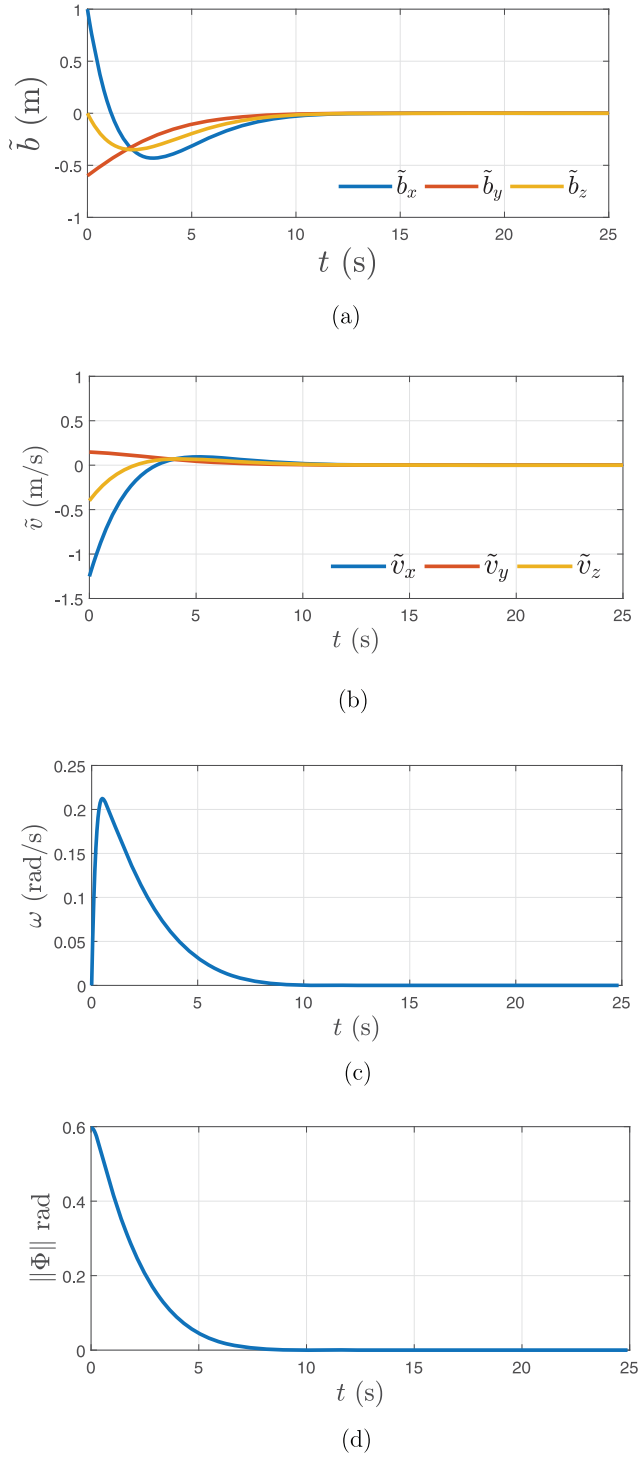

Figure 6. Tracking errors for discrete-time FTS tracking control scheme for $\Delta t = 0.05$ and $t_f = 25$ s. (a) Position tracking error. (b) Velocity tracking error. (c) Angular velocity error. (d) Attitude tracking error function.

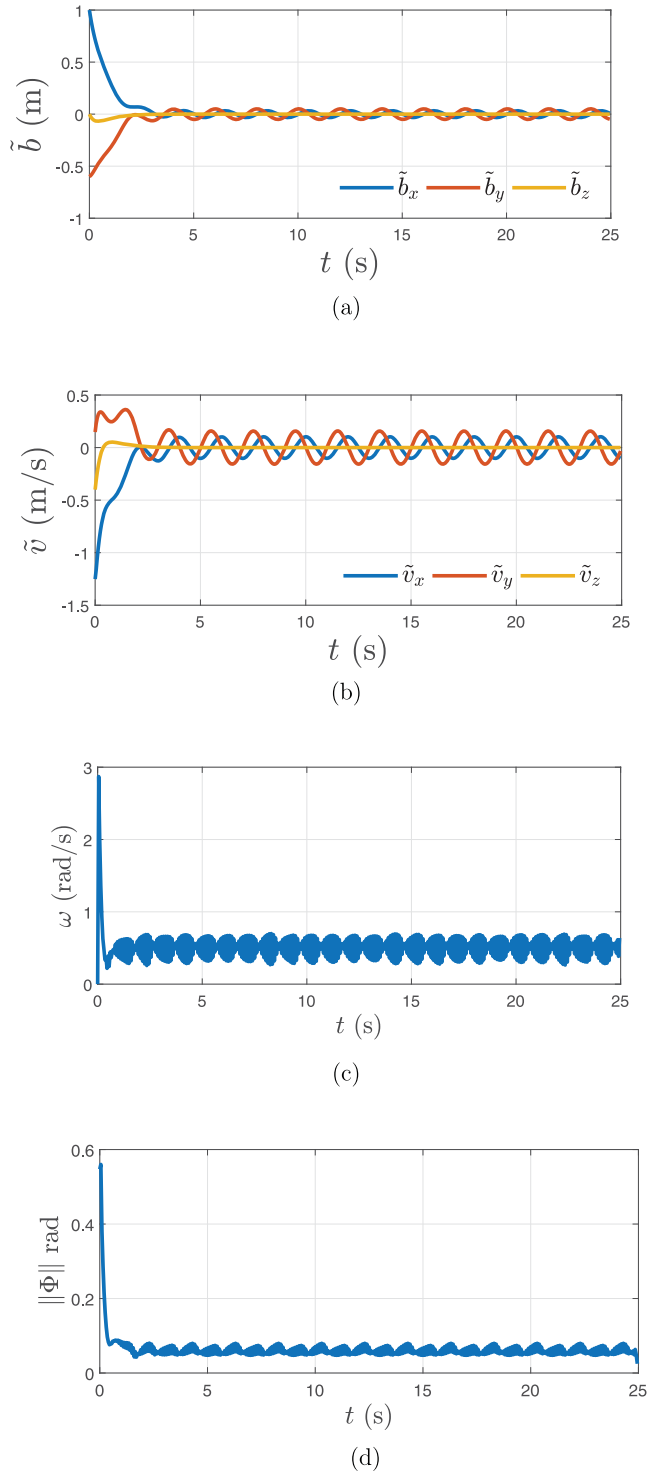

Figure 7. Tracking errors for sampled FTS continuous tracking control scheme for $\Delta t = 0.05$ and $t_f = 25$ s. (a) Position tracking error. (b) Velocity tracking error. (c) Angular velocity error. (d) Attitude tracking error.

difference $\mathbb{V}_{k+1} - \mathbb{V}_k$ as:

$$\Delta \mathbb{V}_{\max} = \max\left[(\mathbb{V}_{k+1} - \mathbb{V}_k) > 0\right], \tag{97}$$

and $\mathbb{V}_k$ denotes the sum of the values of the Lyapunov functions for the position and attitude tracking errors as defined in (35) and (66), respectively. The value of $\mathbb{V}_{k+1} - \mathbb{V}_k$ is expected to be negative for a finite-time stable system until it converges to zero in finite time, which ensures the stability of the system in finite time. On the contrary, a significant increase in the value of $\Delta \mathbb{V}_{\max}$ occurs for the sampled continuous FTS tracking scheme as time step size increases, whereas $\Delta \mathbb{V}_{\max}$ has a negligible value (to machine precision) when the discrete-time FTS tracking control scheme is implemented.

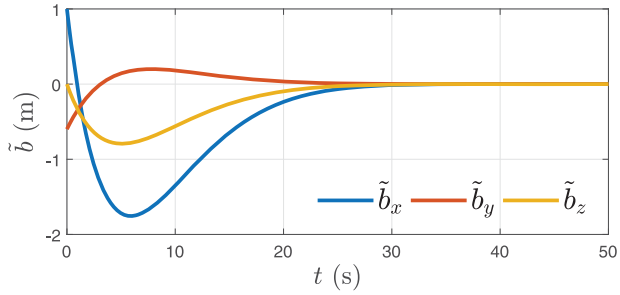

(a)

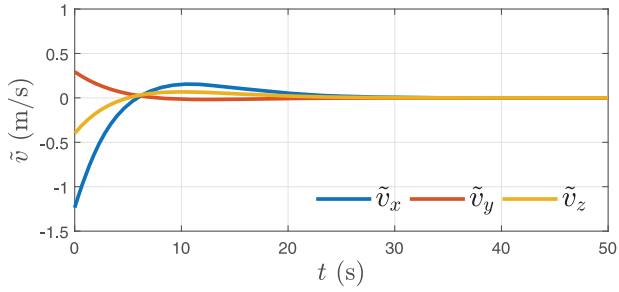

(b)

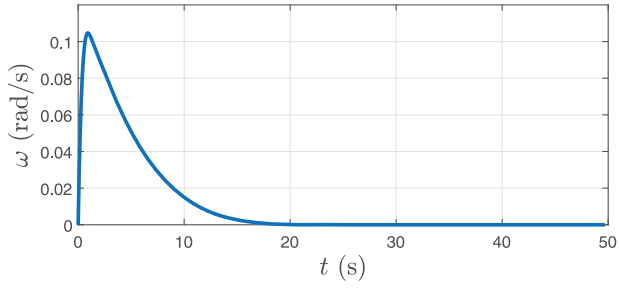

(c)

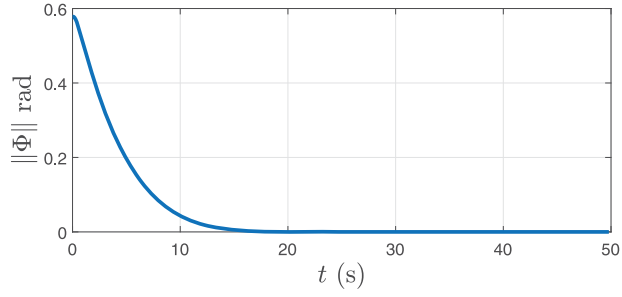

(d)

Figure 8. Tracking errors for discrete-time FTS tracking control scheme for $\Delta t = 0.1$ and $t_f = 50$ s. (a) Position tracking error. (b) Velocity tracking error. (c) Angular velocity error. (d) Attitude tracking error function.

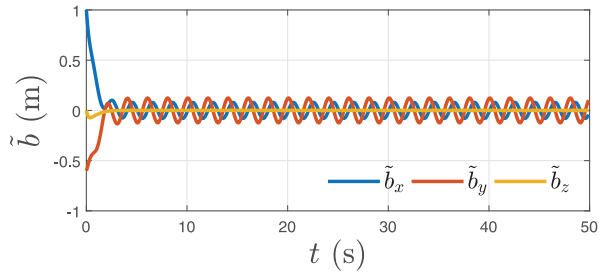

(a)

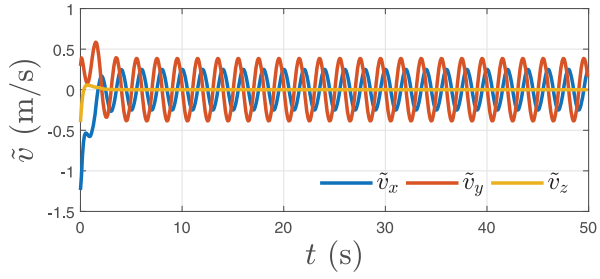

(b)

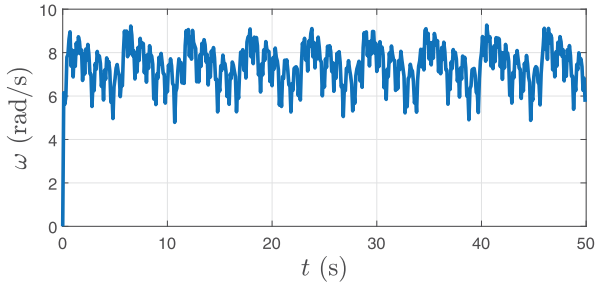

(c)

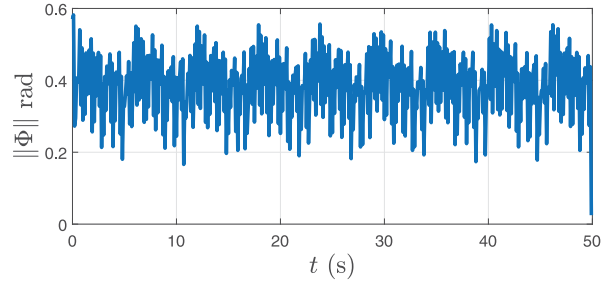

(d)

Figure 9. Tracking errors for sampled FTS continuous tracking control scheme for $\Delta t = 0.1$ and $t_f = 50$ s. (a) Position tracking error. (b) Velocity tracking error. (c) Angular velocity error. (d) Attitude tracking error function.

9. Conclusion

This article proposes a discrete-time stable tracking control scheme with finite-time stability for unmanned vehicles that can be modelled as rigid bodies with one degree of freedom of translational motion and three degrees of freedom of rotational motion actuated. This control scheme is designed with two loops: an inner loop for attitude control and an outer loop for position control. In the outer loop, given a desired position trajectory in an inertial coordinate frame, the desired control force vector is obtained in discrete time to stabilise the desired trajectory in finite time. This control force vector expressed in the body-fixed frame is then used to generate a desired attitude trajectory. In the inner loop to track this desired attitude trajectory, a discrete-time finite-time stable (FTS) attitude tracking scheme is developed and utilised. The outer loop for position tracking

Table 1. Stability performance of discrete-time FTS vs. sampled continuous-time FTS tracking control scheme on SO(3).

Tracking control scheme	$\Delta t(s)$	$t_f(s)$	$\Delta \mathbb{V}_{\max}$
Discrete-time FTS	0.01	5	1.0991×10^{-15}
	0.05	25	4.0776×10^{-25}
	0.1	50	4.1364×10^{-25}
Sampled Continuous FTS	0.01	5	2.3153×10^{-5}
	0.05	25	0.3166
	0.1	50	1.7888

also uses a discrete-time FTS control scheme. The finite-time stability of the overall tracking control scheme is proved using a discrete-time Lyapunov analysis, which results in discrete-time error dynamics in terms of translational and rotational motion tracking errors. A two-step method is proposed for each of the two control loops here, designed using a Lyapunov function that is quadratic in vector-valued functions linear in velocity and angular velocity tracking errors. Then, it is shown that position and attitude tracking errors converge to zero when this vector-valued function vanishes. This analysis results in discrete-time control laws that guarantee the convergence of the position and attitude states to the desired position and attitude trajectories in a finite time interval. Analysis of robustness to bounded disturbance torque is also presented. Moreover, a comparison between the performance of the proposed scheme and that of a sampled continuous FTS scheme is studied here, and numerical results show that a discrete-time FTS tracking control scheme is more reliable for onboard computer implementation when we need to work with a variety of input data frequencies. Future work will look at a more comprehensive comparison of the proposed discrete-time stable tracking control scheme with other state-of-the-art sampled continuous-time tracking control schemes. Further, results of indoor flight experiments on a quadrotor unmanned aerial vehicle will be provided to verify the practical performance of the proposed discrete-time FTS tracking control scheme in comparison to those of sampled continuous-time schemes.

Acknowledgments

The authors acknowledge support from the National Science Foundation award CISE 1739748.

Disclosure statement

No potential conflict of interest was reported by the author(s).

Funding

The authors acknowledge support from the National Science Foundation award CISE 1739748.

References

Bhat, S. P., & Bernstein, D. S. (1998, May). Continuous finite-time stabilization of the translational and rotational double integrators. *IEEE Transactions on Automatic Control*, *43*(5), 678–682. https://doi.org/10.1109/9.668834

Bhat, S. P., & Bernstein, D. S. (2000). Finite-time stability of continuous autonomous systems. *SIAM Journal on Control and Optimization*, *38*(3), 751–766. https://doi.org/10.1137/S0363012997321358

Bohn, J., & Sanyal, A. K. (2015). Almost global finite-time stabilization of rigid body attitude dynamics using rotation matrices. *International Journal of Robust and Nonlinear Control*, *26*(9), 2008–2022. https://doi.org/10.1002/rnc.v26.9

Bullo, F., & Murray, R. M. (1999). Tracking for fully actuated mechanical systems: A geometric framework. *Automatica*, *35*(1), 17–34. https://doi.org/10.1016/S0005-1098(98)00119-8

Chaturvedi, N. A., Sanyal, A. K., & McClamroch, N. H. (2011, June). Rigid-body attitude control. *IEEE Control Systems Magazine*, *31*(3), 30–51. https://doi.org/10.1109/MCS.2011.940459

Dorato, P. (2006). An overview of finite-time stability. In *Current trends in nonlinear systems and control: In honor of Petar Kokotović and Turi Nicosia* (pp. 185–194). Birkhäuser, Boston.

Fernando, T., Chandiramani, J., Lee, T., & Gutierrez, H. (2011). Robust adaptive geometric tracking controls on SO(3) with an application to the attitude dynamics of a quadrotor UAV. In *2011 50th IEEE conference on decision and control and European control conference* (pp. 7380–7385). IEEE.

Goodarzi, F. A., Lee, D., & Lee, T. (2015). Geometric control of a quadrotor UAV transporting a payload connected via flexible cable. *International Journal of Control, Automation and Systems*, *13*, 1486–1498. https://doi.org/10.1007/s12555-014-0304-0

Haddad, W. M., Nersesov, S. G., & Du, L. (2008, June). Finite-time stability for time-varying nonlinear dynamical systems. In *2008 American control conference* (pp. 4135–4139). IEEE.

Hamrah, R., Sanyal, A. K., & Prabhakaran, S. (2019). Discrete finite-time stable position tracking control of unmanned vehicles. In *58th IEEE conference on decision and control (CDC)*. IEEE. Dec. 2019

Hamrah, R., Sanyal, A. K., & Prabhakaran, S. (2020). Discrete Finite-time Stable Attitude Tracking Control of Unmanned Vehicles on SO(3). 2020 American Control Conference (ACC), Jul. 2020. IEEE.

Hamrah, R., Warier, R. R., & Sanyal, A. K. (2018). Discrete-time stable tracking control of underactuated rigid body systems on SE(3). In *57th IEEE conference on decision and control, CDC 2018* (pp. 2932–2937). Dec. 2018. IEEE.

Harshavarthini, S., Rathinasamy, S., & Ahn, C. (2019). Finite-time reliable attitude tracking control design for nonlinear quadrotor model with actuator faults. *Nonlinear Dynamics*, *96*(4), 2681–2692. https://doi.org/10.1007/s11071-019-04952-4

Hussein, I. I., Leok, M., Sanyal, A. K., & Bloch, A. M. (2006). A discrete variational integrator for optimal control problems on SO(3). In *IEEE conference on decision and control (CDC)* (pp. 6636–6641). IEEE.

Invernizzi, D., & Lovera, M. (2017). Geometric tracking control of a quadcopter tiltrotor UAV. *IFAC-PapersOnLine*, *50*(1), 11565–11570. (*20th IFAC world congress*). https://doi.org/10.1016/j.ifacol.2017.08.1645

Izadi, M., Samiei, E., Sanyal, A. K., & Kumar, V. (2015). Comparison of an attitude estimator based on the Lagrange-d'Alembert principle with some state-of-the-art filters. In *2015 IEEE international conference on robotics and automation (ICRA)*. IEEE.

Izadi, M., & Sanyal, A. K. (2014). Rigid body attitude estimation based on the Lagrange–d'Alembert principle. *Automatica*, *50*(10), 2570–2577. https://doi.org/10.1016/j.automatica.2014.08.010

Izadi, M., & Sanyal, A. K. (2016). Rigid body pose estimation based on the Lagrange–d'Alembert principle. *Automatica*, *71*, 78–88. https://doi.org/10.1016/j.automatica.2016.04.028

Kushleyev, A., Mellinger, D., Powers, C., & Kumar, V. (2013). Towards a swarm of agile micro quadrotors. *Autonomous Robots*, *35*(4), 287–300. https://doi.org/10.1007/s10514-013-9349-9

Lee, H., Kim, S., Ryan, T., & Kim, H. J. (2013). Backstepping control on SE(3) of a micro quadrotor for stable trajectory tracking. In *2013 IEEE international conference on systems, man, and cybernetics* (pp. 4522–4527). IEEE.

Lee, D., Kim, H. J., & Sastry, S. (2009). Feedback linearization vs. adaptive sliding mode control for a quadrotor helicopter. *International Journal of Control, Automation and Systems*, *7*, 419–428. https://doi.org/10.1007/s12555-009-0311-8

Lee, T., Leok, M., & McClamroch, N. H. (2005). A Lie group variational integrator for the attitude dynamics of a rigid body with applications to the 3D pendulum. In *IEEE conference on control applications* (pp. 962–967). IEEE.

Lee, T., Leok, M., & McClamroch, N. H. (2010). Geometric tracking control of a quadrotor UAV on SE(3). In *49th IEEE conference on decision and control (CDC)* (pp. 5420–5425). IEEE.

Lee, T., Leok, M., & McClamroch, N. H. (2012). Nonlinear robust tracking control of a quadrotor UAV on SE(3). In *2012 American control conference (ACC)* (pp. 4649–4654). IEEE.

Marsden, J. E., & West, M. (2001). Discrete mechanics and variational integrators. *Acta Numerica*, *10*, 357–514. https://doi.org/10.1017/S096249290100006X

Mellinger, D., & Kumar, V. (2011). Minimum snap trajectory generation and control for quadrotors. In *2011 IEEE international conference on robotics and automation* (pp. 2520–2525). IEEE.

Mellinger, D., Michael, N., & Kumar, V. (2012). Trajectory generation and control for precise aggressive maneuvers with quadrotors. *The International Journal of Robotics Research*, *31*(5), 664–674. https://doi.org/10.1177/0278364911434236

Nordkvist, N., & Sanyal, A. K. (2010). A Lie group variational integrator for rigid body motion in SE(3) with applications to underwater vehicle dynamics. In *49th IEEE conference on decision and control (CDC)* (pp. 5414–5419). IEEE.

Prabhakaran, S., Sanyal, A. K., & Izadi, M. (2017). Integrated guidance and nonlinear feedback control of underactuated unmanned aerial vehicles in SE(3). In *AIAA guidance, navigation, and control conference, AIAA SciTech forum*. AIAA.

Prabhakaran, S., A. K. Sanyal, & Samiei, E. (2018). Integrated guidance and feedback control of underactuated robotics system in SE(3). *Journal of Intelligent and Robotic Systems*, *89*(1–2), 251–263. https://doi.org/10.1007/s10846-017-0547-0

Prabhakaran, S., Sanyal, A. K., & Warier, R. R. (2017). Finite-time stable tracking control for a class of underactuated aerial vehicles in SE(3). In *2017 American control conference, ACC 2017* (pp. 3926–3931). May 2017. IEEE.

Rudin, K., Hua, M., Ducard, G., & Bouabdallah, S. (2011, August 28–September 2). A robust attitude controller and its application to quadrotor helicopters. In *18th IFAC world congress* (pp. 10379–10384). Elsevier.

Sanyal, A. K. (2019). *Nonlinearly stable real-time learning and model-free control*. Preprint. arXiv:1907.10840.

Sanyal, A. K., & Bohn, J. (2015). Finite-time stabilisation of simple mechanical systems using continuous feedback. *International Journal of Control*, *88*(4), 783–791. https://doi.org/10.1080/00207179.2014.974675

Sanyal, A. K., Bohn, J., & Bloch, A. M. (2013, December). Almost global finite time stabilization of rigid body attitude dynamics. In *52nd IEEE conference on decision and control* (pp. 3261–3266). IEEE.

Sanyal, A. K., & Chaturvedi, N. A. (2008). Almost global robust attitude tracking control of spacecraft in gravity. In *AIAA guidance, navigation and control conference and exhibit*. American Institute of Aeronautics and Astronautics Inc.

Sanyal, A. K., Nordkvist, N., & Chyba, M. (2011). An almost global tracking control scheme for maneuverable autonomous vehicles and its discretization. *IEEE Transactions on Automatic Control*, *56*, 457–462. https://doi.org/10.1109/TAC.2010.2090190

Shi, X. N., Zhang, Y. A., & Zhou, D. (2015). A geometric approach for quadrotor trajectory tracking control. *International Journal of Control*, *88*(11), 2217–2227. https://doi.org/10.1080/00207179.2015.1039593

Varadarajan, V. (1984). Lie Groups and Lie Algebras. Lie Groups, Lie Algebras, and Their Representations, pp.41–148. https://doi.org/10.1007%2F978-1-4612-1126-6_2.

Wang, L., He, Y., Zhang, Z., & He, C. (2013). Trajectory tracking of quadrotor aerial robot using improved dynamic inversion method. *Intelligent Control and Automation*, *4*(4), 343–348. https://doi.org/10.4236/ica.2013.44040

Yan, Z., Yu, H., Zhang, W., Li, B., & Zhou, J. (2015). Globally finite-time stable tracking control of underactuated UUVs. *Ocean Engineering*, *107*, 132–146. https://doi.org/10.1016/j.oceaneng.2015.07.039